

This discussion paper is/has been under review for the journal Atmospheric Chemistry and Physics (ACP). Please refer to the corresponding final paper in ACP if available.

# Simulation of the mineral dust content over Western Africa with the CHIMERE-DUST model from the event to the annual scale

C. Schmechtig<sup>1</sup>, B. Marticorena<sup>1</sup>, B. Chatenet<sup>1</sup>, G. Bergametti<sup>1</sup>, and J. L. Rajot<sup>2</sup>

<sup>1</sup>LISA, UMR CNRS 7583, Universités Paris Est-Paris Diderot, Créteil, France

<sup>2</sup>IRD-UMR 211 BIOEMCO, Niamey, Niger

Received: 17 December 2010 – Accepted: 19 January 2011 – Published: 9 March 2011

Correspondence to: C. Schmechtig (schmechtig@lisa.u-pec.fr)

Published by Copernicus Publications on behalf of the European Geosciences Union.

ACPD

11, 8027–8079, 2011

## Simulation of the mineral dust content over Western Africa

C. Schmechtig et al.

Title Page

Abstract

Introduction

Conclusions

References

Tables

Figures

⏪

⏩

◀

▶

Back

Close

Full Screen / Esc

Printer-friendly Version

Interactive Discussion



## Abstract

The chemistry and transport model CHIMERE-Dust have been used to simulate the mineral dust cycle over the Sahara in 2006. Surface measurements deployed during the AMMA field campaign allows to test the capability of the model to correctly reproduce the atmospheric dust load and surface concentrations from the daily to the seasonal time-scale. The seasonal pattern simulated for Aerosol Optical Depth and surface concentrations are in good agreement with observations. The simulated daily concentrations and hourly AOD are in the same range than the observed one despite relatively high simulated dust emissions. At the different time-scales, the quantitative agreement between the simulations and the observations is fairly good. The capability of the model to reproduce the altitude of the dust transport was tested for two contrasted cases of low and high altitude transport. These results highlights the sensitivity of the simulations to the surface winds used as external forcing and the necessity to further constrain the dust mass budget at the regional scale.

## 1 Introduction

Mineral dust, mainly produced by the aeolian erosion occurring in arid and semiarid regions, represents about 40% of the aerosol mass emitted annually into the troposphere (IPCC, 2007). Most of the recent studies on mineral dust focus on their radiative effects and thus on their contribution to the expected climate changes. Indeed, during their transport in the atmosphere, mineral dust can cause either a positive or a negative radiative effect leading to a warming or cooling of the atmospheric layers (Sokolik et al., 2001), depending on both the surface characteristics and the optical properties of dust (Tegen and Lacis, 1996). These particles are also involved in chemical heterogeneous processes, interacting for example with nitrous (Manabe and Gotlieb, 1992; Wu and Okada, 1994), sulphured species (Dentener et al., 1996) or with other particles, modifying their chemical composition (Zhao et al., 1988), their size distribution and/or

## Simulation of the mineral dust content over Western Africa

C. Schmechtig et al.

Title Page

Abstract

Introduction

Conclusions

References

Tables

Figures



Back

Close

Full Screen / Esc

Printer-friendly Version

Interactive Discussion



their number. Finally, when deposited in remote oceanic ecosystems, mineral dust can affect the biogeochemical cycle of some key nutrients or micronutrients such as iron or phosphorus, (Jickells et al., 2005; Mahowald and al., 2008).

The whole dust cycle, i.e. the emission, transport and deposition, is strongly controlled by meteorological parameters, mainly wind and precipitation. For example, N'Tchayi et al. (1994) showed that the number of days the horizontal visibility is affected by dust in Gao (Mali) increased from 20 days to 250 days by year during the Sahelian drought (from 1957 to 1984). Simultaneously, the dust load reaching Barbados, in the western Atlantic Ocean, was multiplied by a factor of four (Prospero and Nees, 1977, 1986). Moulin et al. (1997) showed that inter-annual variations of dust transport from the Sahara-Sahel region towards the Mediterranean Sea and the Atlantic Ocean were connected with the North Atlantic Oscillation Index.

As a result, climatic changes of anthropogenic or natural origins are expected to significantly impact dust emissions and in particular the localisation and intensity of the dust sources.

Because of the high spatial and temporal variability of the dust concentrations in the atmosphere, regional modelling is frequently used to represent the mineral dust cycle and to quantify their impacts. Indeed, if global climatic models tend to reproduce satisfyingly the order of magnitude of the dust load at the global scale and their seasonal cycle (Tegen and Fung, 1994; Ginoux et al., 2001), they do not capture the spatial and temporal variability of atmospheric dust contents at a daily scale or at an inter-annual scale. In addition, they generally fail in representing correctly the seasonal dust cycle of mineral dust over the Sahara and the Sahel (Yoshioka et al., 2005). Chemistry Transport Models (CTMs) forced by meteorological fields provided by global models (e.g. from the European Centre for Medium-range Weather Forecasts) are less sensitive to misrepresentation of the dynamics and better agree with observations (Guelle et al., 2000; Luo et al., 2003). However, their accuracy remains limited by their low horizontal and vertical resolutions.

## Simulation of the mineral dust content over Western Africa

C. Schmechtig et al.

Title Page

Abstract

Introduction

Conclusions

References

Tables

Figures

⏪

⏩

◀

▶

Back

Close

Full Screen / Esc

Printer-friendly Version

Interactive Discussion



---

**Simulation of the mineral dust content over Western Africa**C. Schmechtig et al.

---

[Title Page](#)[Abstract](#)[Introduction](#)[Conclusions](#)[References](#)[Tables](#)[Figures](#)[⏪](#)[⏩](#)[◀](#)[▶](#)[Back](#)[Close](#)[Full Screen / Esc](#)[Printer-friendly Version](#)[Interactive Discussion](#)

5 Simulations based on better resolved mesoscale meteorological models (i.e., Tegen et al., 2006; Bouet et al., 2007; Heinold et al., 2007; Tulet et al., 2008; Bou Karam et al., 2009) allows a more accurate description of the dynamics processes involved in the mineral dust cycle. However, these modelling tools are time-consuming and thus are  
10 mainly used for the simulations of case-studies. As an example, Heinold et al. (2007) simulated two major Saharan dust outbreaks transported towards Europe in August and October 2001 with the LM-MUSCAT dust model while Bouet et al. (2007) simulated the surface measurements from the BoDEx Experiment with the RAMS (Regional Atmospheric Modelling System) model. More recently, Schepanski et al. (2008) investigated the Saharan dust transport and deposition toward the Atlantic Ocean based on  
15 three months of simulation with the LM-MUSCAT dust model.

An alternative to investigate longer time periods over a specific region is to use a regional CTM, i.e. a CTM externally forced by regional meteorological fields. Such modelling tool have been widely developed and used to perform 3-D regional simu-  
20 lations of the tropospheric chemical composition because chemical models are extremely time consuming. Developed on the basis of the CTM CHIMERE (Vautard et al., 2001; Bessagnet et al., 2004), the CHIMERE-DUST model, is a dust-dedicated modelling tool which allows performing multi-annual simulations with a relevant spatial and temporal scale. This model was tested for dust forecasting during the winter  
25 2006, including the dry-season experimental phase (SOP0) of the international African Monsoon Multidisciplinary Analysis (AMMA) program (Menut et al., 2009). A detailed description of the model can be found in Menut et al. (2007) and is summarized in Sect. 2.1.

Using this model to investigate the variability of the mineral dust content over West Africa requires first a careful evaluation of its capability to simulate the main characteristic of the dust distribution, from the emission intensity and source location to transport patterns.

As highlighted by many authors (i.e. Jaenicke and Schütz, 1978; d'Almeida and Schütz, 1983) the size range respectively covered by the mass and the number dust

size distributions are very different. As an example, using a size distribution typical of emission conditions (emission by an aluminosilicate silt soil type (ASS) under a wind friction velocity  $U_*$  of  $55 \text{ cm s}^{-1}$  derived from Alfaro and Gomes, 20001), Forêt et al. (2006) estimated that particles with diameters greater than  $2 \mu\text{m}$  represent 98% of the mass distribution while they account for only 12% of the number distribution. These differences in the contribution of the different size range to the mass and to the number distribution significantly impact the way 3-D models can be tested, validated or optimized against observations. Cakmur et al. (2005) tried to constrain the magnitude of the dust emissions by using multiple observational data set. They showed that the magnitude of the dust cycle is very sensitive to the data set used as a constraint, if only one data set is chosen. Typically, the results of their optimization of the dust emissions showed that the dust “clay” fraction (dust size from  $0.01 \mu\text{m}$  to  $1 \mu\text{m}$ ) is mainly constrained by the AOT measurements, while surface concentration and deposition measurements determine the “silt” (dust size from  $1 \mu\text{m}$  to  $10 \mu\text{m}$ ). They indicate that a consensus optimal solution agreeing with all the observations can be identified when using a combination of different data sets.

The data collected during the AMMA international program offered the opportunity to produce such a combination of observations. The main objective of the AMMA is to improve our knowledge and understanding of the West African Monsoon (WAM) and its variability, with an emphasis on daily-to-interannual time scales (Redelsperger et al., 2006). In the framework of this program, a set of 3 ground-based measurement stations located between  $13\text{--}14^\circ \text{N}$ , the so-called “Sahelian Dust Transect” (SDT), has been deployed during 3 yr. It includes measurements of the  $\text{PM}_{10}$  (Particulate Matter collected with a cut-off  $50\% = 10 \mu\text{m}$  in diameter) concentration at the surface and of the column-integrated aerosol amount and properties, i.e. the aerosol optical depth (Marticorena et al., 2010).

In this study, we compare the simulations performed with the CHIMERE-DUST model with the measurements performed in 2006, i.e. the year the intensive experimental phase of the AMMA program took place. After a presentation of the model,

## Simulation of the mineral dust content over Western Africa

C. Schmechtig et al.

[Title Page](#)[Abstract](#)[Introduction](#)[Conclusions](#)[References](#)[Tables](#)[Figures](#)[◀](#)[▶](#)[◀](#)[▶](#)[Back](#)[Close](#)[Full Screen / Esc](#)[Printer-friendly Version](#)[Interactive Discussion](#)

the measurements and the simulated dust emissions, the capability of the model to retrieve the seasonal dust cycle of the atmospheric dust load and the main characteristics of two typical dust events will be evaluated. This evaluation will be based on a comparison between the simulated and measured AOD and between concentrations simulated in the first layer of the model and the surface concentrations measured along the Sahelian Dust transect.

## 2 Tools and methods

### 2.1 CHIMERE-DUST model

#### 2.1.1 Simulation domain and time period

The simulation runs on a large domain ( $10^{\circ}$  S– $60^{\circ}$  N,  $90^{\circ}$  W– $90^{\circ}$  E) including the North of Africa and the North Tropical Atlantic Ocean. This large domain allows to investigate dust transport from the Sahara and the Sahel towards the Atlantic Ocean and/or the Mediterranean Sea. Because of its size, the horizontal domain has a horizontal grid resolution of  $1^{\circ} \times 1^{\circ}$ . Vertically, 15 levels are defined from the surface to 12 km (i.e. 200 hPa), the first layer of the model extending from 0 to 54 m. Turbulent parameters as,  $U_*$ , the friction velocity and,  $h$ , the boundary layer depth are estimated from the mean meteorological parameters (the wind components,  $u$  and  $v$ , the temperature  $T$ , the specific humidity  $q$ , and the pressure  $p$ ).

The transport model is that of the chemistry-transport model CHIMERE (Vautard et al., 2001; Bessagnet et al., 2004) currently used for boundary layer regional air pollution studies and forecast. The horizontal transport is performed using the Van Leer scheme (Van Leer, 1979), the vertical transport with the first-order upwind scheme and the vertical mixing is estimated from the calculation of the bulk Richardson number as extensively described in Menut (2003). There is no added numerical horizontal diffusion considering that the transport scheme is diffusive enough. The dust simulations

## Simulation of the mineral dust content over Western Africa

C. Schmechtig et al.

Title Page

Abstract

Introduction

Conclusions

References

Tables

Figures

◀

▶

◀

▶

Back

Close

Full Screen / Esc

Printer-friendly Version

Interactive Discussion



are performed with a one hour time-step for the whole year 2006. Typically, using a standard single processor machine, a one year simulation requires one week of computation.

### 2.1.2 Dust emissions model

Dust emissions are computed over the Sahara and the Arabian Peninsula using the dust emission model developed by Marticorena and Bergametti (1995). This model described the main step of the dust emission processes, i.e. the erosion threshold, the saltation flux and the dust emission efficiency, as a function of the local surface roughness and of the soil size-distribution. The dust emission efficiency data set used for the simulations is the re-evaluation of the Marticorena et al.'s (1997) proposed by Laurent et al. (2008).

This emission model requires a mapping of surface properties (aeolian roughness lengths, soil types, soil textures). We use the surface data bases established according to Marticorena et al. (1997) and Callot et al. (2000) that includes the Sahara desert, but extended to the Arabian Peninsula, Middle East and Minor Asia. The spatial resolution of the data base is  $1^\circ \times 1^\circ$ , but, up to 5 different surface features (i.e. five combinations of soil type, surface roughness and fraction of erodible surface) can be distinguished in each square degree. This method operates like a Geographical Information System (GIS) by aggregating refined data deduced from various sources of information (topographical, geological maps, etc.,...) to a larger scale and more general information (Callot et al., 2000). The main support used for this mapping are the topographic maps from the French National Geographic Institut (IGN) available at various spatial scales (1/200 000; 1/500 000; 1/1 000 000) over the Sahara, the Soviet Military Topographic Maps (1/200 000; 1/500 000) over the Arabian Peninsula and the 1/250 000 American Maps (J.O.G.) from the Army Map Service of the US Army (1957–1958) for Minor Asia or the South eastern Sahara.

## Simulation of the mineral dust content over Western Africa

C. Schmechtig et al.

Title Page

Abstract

Introduction

Conclusions

References

Tables

Figures



Back

Close

Full Screen / Esc

Printer-friendly Version

Interactive Discussion



### 2.1.3 Dust size distribution

The size distribution of the emitted dust is computed according to the Alfaro and Gomes (2001) and Alfaro et al. (2004) model. This simulated dust size distribution is a combination of three log-normal distributions (Mode 1:  $D_{\text{med}1} = 1.5 \mu\text{m}$ ,  $\sigma_1 = 1.7$ ; Mode 2:  $D_{\text{med}2} = 6.7 \mu\text{m}$ ,  $\sigma_2 = 1.6$ ; Mode 3:  $D_{\text{med}3} = 14.2 \mu\text{m}$ ,  $\sigma_3 = 1.6$ ) whose relative proportions vary as a function of the soil type and of the wind friction velocity. Three different initial mass size distributions, resulting from different soil types and wind friction velocities taken from Alfaro and Gomes (2001) are given as examples on Fig. 1. The mass size distribution corresponding to a dust size distribution dominated by mode 1 (83%) is produced from a coarse soil (Coarse Sand) for a high wind friction velocity ( $U_* = 80 \text{ cm s}^{-1}$ ). The coarser dust size distribution, composed of 95% of the Mode 3, is produced from a fine soil (Alumino silicated silt) at low wind friction velocity ( $U_* = 35 \text{ cm s}^{-1}$ ). An intermediate case with 10% of Mode 1, 18% of Mode 2 and 78% of Mode 3, produced by a coarse sand (CS) at a moderate wind friction velocity ( $U_* = 40 \text{ cm s}^{-1}$ ), is also presented.

The vertical dust fluxes estimated from the dust emission efficiencies are then redistributed into the model size bins using a mass partition scheme. The dust size distribution is represented using 20 iso-log bins ranging from 0.01 to 24  $\mu\text{m}$ . This number of bins is sufficiently high to avoid any bias in the simulation of the dust mass concentration, deposition and optical depth (Forêt et al., 2006).

### 2.1.4 Dust deposition

Dry deposition velocity is computed as a function of particle diameter following Venkatram and Pleim (1999). These authors proposed a slightly modified version of the formulation initially proposed by Wesely (1989). This dry deposition scheme introduces little differences in the magnitude of the deposition velocity but has the advantages to be consistent with the mass conservation equation and to be theoretically more accurate for large particles (Menuet et al., 2007).

## Simulation of the mineral dust content over Western Africa

C. Schmechtig et al.

Title Page

Abstract

Introduction

Conclusions

References

Tables

Figures

◀

▶

◀

▶

Back

Close

Full Screen / Esc

Printer-friendly Version

Interactive Discussion



Wet removal processes includes two distinct mechanisms: rainout corresponds to the in-cloud scavenging of particles acting as condensation nuclei while wash-out refers to the below cloud scavenging of particles impacting by falling rain droplets. Due to their composition, dust particles are often considered as purely hydrophobic so no in-cloud scavenging is considered. This is also the case for CHIMERE-dust. Below-cloud scavenging is parameterized according to Slinn (1984) modified by Loosmore and Cederwall (2004) to account for larger scavenging in heavy rain events.

### 2.1.5 Meteorological fields

The model is forced by 3-D meteorological fields from the European Centre for Medium Weather Forecast (ECMWF). The used meteorological products are the “first guess” forecast products, i.e. almost similar to the operational analysis, at  $1^\circ \times 1^\circ$  resolution and every 3 h. This spatial resolution allows to perform the simulation over the selected large geographical domain during one year with an hourly temporal resolution.

It is now well recognized that the large scale meteorological models fail in reproducing the surface wind velocity in the Bodélé depression (Chad), one of the most active Saharan dust sources. Koren and Kaufman (2004) showed that NCEP (National Centre for Environmental Prediction) reanalysis winds underestimate by factor 2 the actual speed of the dust front in this region. Similarly, Bouet et al. (2007) found that ECMWF wind surface reanalysis are significantly underestimated compare to the surface wind locally measured in Chicha (Chad) in March 2005 during the the BoDEx 2005 experiment (Washington et al., 2006). In order to improve the dust emission simulations over the Bodélé depression, the 10 m surface winds measured in Faya-Largeau were compared with the ECMWF surface winds in the corresponding model grid mesh for the period January to March 2004, a period during which a sufficient number of observations is available both during day and night (Fig. 2). This period is known as a dusty period and several severe dust events occurred, in particular in early March (Menut et al., 2007). The comparison between the surface measurements and the ECMWF surface winds shows a similar temporal pattern. However, the amplitude of the diurnal

## Simulation of the mineral dust content over Western Africa

C. Schmechtig et al.

Title Page

Abstract

Introduction

Conclusions

References

Tables

Figures



Back

Close

Full Screen / Esc

Printer-friendly Version

Interactive Discussion



cycle is lower in the ECMWF winds than in the measurements, leading to a systematic underestimation of the highest winds. The measured surface wind velocities are as high as  $20 \text{ m s}^{-1}$  while surface wind velocities from ECMWF never exceed  $12 \text{ m s}^{-1}$ . Regarding the importance of the Bodélé depression as a dust source, a correction of the ECMWF surface wind was applied based on a linear fit ( $r^2 = 0.79$ ;  $n = 97$ ) between the measured and modelled surface winds in Faya-Largeau (Fig. 3):

$$10 \text{ m WindSpeed}_{\text{corrected}} = -4,62707 + 1,7496 \times 10 \text{ m WindSpeed}_{\text{ECMWF}} \quad (1)$$

This correction is systematically applied to the grid meshes between  $15^\circ \text{ N}$ – $19^\circ \text{ N}$  and  $15^\circ \text{ E}$ – $20^\circ \text{ E}$  corresponding to the Bodélé depression. Since this correction is not a simple ratio, it does not systematically lead to an increase of the surface wind velocities. In particular, it increases the amplitude of the diurnal cycle, in agreement with measurements. It must be noted that this correction lead to surface winds that remains lower than those recorded at the station of Faya largeau (Fig. 2). This correction produces an increase of the surface winds only for initial surface winds higher than the erosion threshold. As a result, it does not change the occurrence of the dust events but only their intensity. The impact of this correction on the simulated dust emissions will be discussed later.

### 2.1.6 Aerosol optical depth

The aerosol optical depth at the reference solar wavelength of 550 nm is computed by a vertical integration of the simulated dust mass concentration  $C$  in each size bin weighted by the specific surface extinction mass,  $\sigma_e$  calculated based on the Mie theory with a dust refractive index of  $(1.5-0.005i)$  (Moulin et al., 2001):

$$\text{AOD} = \int_0^{\text{TOA}} \sigma_e(z) C(z) dz \quad (2)$$

## Simulation of the mineral dust content over Western Africa

C. Schmechtig et al.

Title Page

Abstract

Introduction

Conclusions

References

Tables

Figures

◀

▶

◀

▶

Back

Close

Full Screen / Esc

Printer-friendly Version

Interactive Discussion



$$\text{AOD} = \int_0^{\text{TOA}} \sum_i^{\text{Nbin}} \sigma_e(z, i) C(z, i) dz \quad (3)$$

Since the extinction is maximum for particle diameter of about 0.55  $\mu\text{m}$ , the most optically active particles in the dust mass size distribution comes from Mode 1. As a consequence, for the size distributions illustrated in Fig. 1 and for the same mass concentration, the finest size distribution would produce an AOD higher by a factor of 10 than the coarser one. In fact, once the mass proportion of Mode 1 exceeds 10%, more than 50% of the AOD is due to particles smaller than 3  $\mu\text{m}$ . As a result, AOD measurements in the visible range allow to test the capability of the model to simulate the most active dust particles on a radiative point of view. But they do not necessarily provide a sufficient level of constraint on the total atmospheric dust load and in particular on the contribution of the coarse dust particles to the total mass.

## 2.2 The Sahelian Dust Transect

The acquisition of quantitative information on the mineral dust content over the Sahel was the main objective of the deployment of the “Sahelian Dust Transect” (SDT) (Marticorena et al., 2010). This transect is composed of three stations aligned between 13 and 14° N along the main pathway of the Saharan and Sahelian dust toward the Atlantic Ocean, namely Banizoumbou (Niger, 13.54° N, 2.66° E), Cinzana (Mali, 13.28° N, 5.93° W) and M’Bour (Senegal, 14.39° N, 16.96° W). Two of the three stations, Banizoumbou and M’Bour, have been implemented on pre-existing stations of the international network of sunphotometers AERONET (Aerosol Robotic Network) (Holben et al., 2001). The third station, Cinzana, has been included in the AERONET network in the framework of the AMMA project. The Aerosol Optical Depth (AOD) measured by the sunphotometer corresponds to the extinction due to aerosol integrated over the whole atmospheric column. This measurement is thus an indicator of the atmospheric content in optically active particles. AERONET sunphotometers are equipped

## Simulation of the mineral dust content over Western Africa

C. Schmechtig et al.

Title Page

Abstract

Introduction

Conclusions

References

Tables

Figures

◀

▶

◀

▶

Back

Close

Full Screen / Esc

Printer-friendly Version

Interactive Discussion



with different channels allowing to compute the spectral dependence of the AOD, i.e. the Angström coefficient,  $\alpha$ . This spectral dependence is sensitive to the aerosol size. As mentioned above, desert dust is characterized by micron and supermicron particle size modes and thus exhibits very low  $\alpha$  (close to 0), while  $\alpha$  higher than 1 are observed when the aerosol mass size distribution is dominated by submicron particles (Holben et al., 2001). To discriminate the situation where dust clearly dominated the AOD, we selected only the values of AOD for which  $\alpha$  (between 440 and 870 nm) is lower than 0.4 (note that in the following, all presented AODs are AODs for which  $\alpha$  is lower than 0.4). In the model, the AOD is simulated at 550 nm, it is thus compared to the AOD measured at the closest wavelength, 675 nm. Because the  $\alpha$  is close to 0, the difference in the wavelength should not significantly affect the comparison. An estimation of the possible bias can be made by comparing the AOD measured at 675 and 44 nm. For the three stations, the AOD at 675 and 440 nm associated with  $\alpha < 0.4$  are significantly correlated ( $R = 0.99$ ) with slopes ranging from 1.04 in Cinzana to 1.06 in M'Bour. The difference induced by the comparison of modelled AODs at 550 nm and AODs measured at 675 nm should therefore not exceed 6%.

Since January 2006, in addition to the AOD, the SDT provides a continuous monitoring of the atmospheric concentrations of Particulate Matter smaller than  $10\ \mu\text{m}$  ( $\text{PM}_{10}$ ). They are measured at each station with a 5-min time step, using a Tapered Element Oscillating Microbalance (TEOM 1400A from Thermo Scientific) equipped with a  $\text{PM}_{10}$  inlet. The inlet is located at  $\sim 9\ \text{m}$  from the ground level in M'Bour and  $\sim 6\ \text{m}$  in Banizoumbou and Cinzana. Occasionally, aerosol vertical profiles were measured by a one-wavelength micro-lidar (Cavaliere et al., 2011).

As described in Marticorena et al. (2010) a selection of the data is applied to retain only the periods during which mineral dust are the main contributor to the measured  $\text{PM}_{10}$  mass. The procedure consists in excluding data from wind sectors that can bring other aerosol to the stations. This selection is critical for the M'Bour station which is located on the sea side, south of the town of M'Bour ( $\sim 180\ 000$ – $200\ 000$  inhabitants). As a result, data from wind sectors corresponding to transport from the sea or from

## Simulation of the mineral dust content over Western Africa

C. Schmechtig et al.

Title Page

Abstract

Introduction

Conclusions

References

Tables

Figures

◀

▶

◀

▶

Back

Close

Full Screen / Esc

Printer-friendly Version

Interactive Discussion





does not exceed 20%. The difference between the two simulated annual dust emissions cannot thus be due to this factor only. Another element that could explain this difference is the fact that surface wind velocities for the Bodélé Depression have been corrected in order to better reproduce the high surface wind velocities responsible for the spring events. The annual dust emissions simulated for 2006 in the Bodélé Depression region are 227 Tg. Due to the correction emissions from the Bodélé depression are increased by a factor of 10. Despite this correction, dust emissions from this region represent 10% only of the total Saharan dust emissions. This may be considered as relatively low for a region considered by some authors as the most active in the world (Prospero et al., 2002). However, these emissions are not high enough to explain the difference between the two estimations of Saharan dust emissions.

Finally, the observed difference in dust emissions can result from differences in the meteorological surface wind fields used in the two simulations. Laurent et al. (2008) used the ERA-40 data base (not available for the year 2006), while the ECMWF operational products are used in our simulations. We thus compared the surface wind fields from the two data bases for one of the year simulated by Laurent et al. (2008), i.e. 2000 and for the grid meshes where dust emissions are computed. The comparison is made only for wind velocities higher than  $7 \text{ m s}^{-1}$  (i.e.  $\sim$  the minimum modelled 10 m erosion threshold wind velocity) (Fig. 4). In both case the proportion of surface winds exceeding the erosion threshold is very low, 4.5% for the ERA-40 data base and 8.1% for the operational forecast. However, this proportion is 80% higher in the ECMWF operational products than in the ERA-40 data base. So the occurrence of dust emission is potentially 80% higher. Moreover, the surface winds higher than the erosion thresholds are clearly higher in the ECMWF operational products than those from the ERA-40 (Fig. 4). As a result, the simulated dust emissions will be much higher, since dust emission fluxes are computed as a power 3 of the surface wind velocity.

Finally, the use of ECMWF operational products leads to more frequent and more intense dust emissions, which explain the differences between the simulated annual emissions and the one estimated by Laurent et al. (2008). Menut (2007) already

## Simulation of the mineral dust content over Western Africa

C. Schmechtig et al.

Title Page

Abstract

Introduction

Conclusions

References

Tables

Figures



Back

Close

Full Screen / Esc

Printer-friendly Version

Interactive Discussion



highlighted the sensitivity of the dust emission simulations to the surface wind fields. For a 2.5 month period, he found a factor of 3 in the total emissions simulated with ECMWF operational products and with NCEP data base. Here, we found that different meteorological products (operational and re-analysis) from the same meteorological model can also induce a strong difference in the simulated dust emissions.

### 3.1.2 Seasonality of the dust emissions

The simulated dust emissions exhibit a clear seasonal cycle, in agreement with the works of d'Almeida (1986), Marticorena and Bergametti (1996) and Laurent et al. (2008) (Fig. 5). This seasonal cycle is characterized by a maximum of dust emissions during late winter and early spring, a secondary peak being simulated in summer. The minimum dust emissions are simulated for autumn. For 2006, the maximum monthly dust emission are simulated slightly earlier in the year than in Laurent et al. (2008), i.e. in February instead of March. Figure 6 shows that the seasonal cycle of the dust emission is associated with a change in their spatial distribution.

The winter months (January-February-March) (Fig. 6a) exhibit the highest Saharan dust emissions. They are mainly located in the North-east of the Sahara, i.e. in the North of Libya, in the region of the Bodélé depression and in sources located north of Mauritania and Mali. Except for the Libyan sources, these regions were already the most active Saharan dust sources in the simulations performed by Laurent et al. (2008). The Libyan dust emissions are mainly related to an intense dust event simulated by the end of February. At this period, a dust plume is clearly observed on the UV aerosol index images (Herman et al., 1997; Torres et al., 1997) derived from the recent OMI instrument (Ozone Monitoring Instrument) (Fig. 7). The dust event occurs on the 23 February at the frontier between Tunisia and Libya and progress rapidly toward the East to reach Israel on 25 February. At this period, the North of Libya clearly appears as a relatively intense dust source from the seasonal mean AODs derived in the UV (Deep Blue AOD; Hsu et al., 2004, 2006) and OMI aerosol indexes (Fig. 8a).

## Simulation of the mineral dust content over Western Africa

C. Schmechtig et al.

Title Page

Abstract

Introduction

Conclusions

References

Tables

Figures

◀

▶

◀

▶

Back

Close

Full Screen / Esc

Printer-friendly Version

Interactive Discussion



These observations tend to confirm that Libyan sources were active during the winter 2006, but probably overestimated in the simulation.

In spring (April to May), all possible dust sources are activated in the simulation (Fig. 6b). Compared to satellite observations, the simulation exhibits a comparable level of agreement and the same bias than in Laurent et al. (2008): almost all the simulated dust sources correspond either to significant Deep Blue AODs or OMI indexes but some of them appear as similarly overestimated or underestimated in terms of intensity (Fig. 8b). In terms of source location, a slightly better agreement is obtained with the Deep Blue AODs than with the OMI indexes, in particular in the North and Central Sahara. Even if intense emissions are simulated over the region of the Bodélé Depression, their relative intensity compared to the other sources regions is lower in the simulations than in the observations. Except in this region, almost no dust emissions are simulated south of 20° N, while relatively high OMI indexes are recorded. Finally, the dust emissions simulated in the Western Sahara tends to be too intense compared to observations, as already noted by Laurent et al. (2008). Based on the satellite observations, this season should correspond to the period of the maximum of Saharan dust emissions. This suggests again that the winter dust emissions are overestimated in the model.

In the simulations, the summer months correspond to a secondary maximum of Saharan dust emissions (Fig. 8c) and to a shift of the dust sources to the South East part of the Sahara, with very intense emissions along the West Coasts and North of Mauritania and Mali. Such intense dust emissions in the South-western Sahara are consistent with satellite observations, such a pattern being particularly evident from OMI indexes (Fig. 8c).

Autumn (October to December) is the period during which the simulated emissions are the lowest, the region of the Bodélé depression being almost the only intense simulated dust source. Such a spatial pattern perfectly matches with satellite observations and in particular with Deep Blue AOD (Fig. 8d).

## Simulation of the mineral dust content over Western Africa

C. Schmechtig et al.

Title Page

Abstract

Introduction

Conclusions

References

Tables

Figures

◀

▶

◀

▶

Back

Close

Full Screen / Esc

Printer-friendly Version

Interactive Discussion



## 3.2 Dust content over the Sahel

### 3.2.1 Monthly time scale

To test the capability of the model to quantitatively retrieve the seasonal cycle of the mineral dust content in the Sahelian region, the simulated AODs and surface concentrations have been compared to the measurements from the SDT stations.

The order of magnitude of simulated monthly mean AOD are in good agreement with the measurements performed at the three stations and the seasonal variations are also well simulated (Fig. 9). In Banizoumbou, the two AOD maxima measured in March ( $\sim 1$ ) and in June ( $\sim 0.8$ ) in June are well reproduced by the model. Slightly lower maxima are measured in Cinzana, with a higher monthly AOD in June (0.82) than in March (0.7) that are also retrieved in the simulations (0.65 in March and 0.89 in June). In M'Bour the March maximum (0.7) is correctly simulated (0.69) while the June value (0.67) is overestimated in the simulation (1). The AOD measured in January 2006 are strongly underestimated at the three stations. On the opposite, the AODs simulated in November and December at Banizoumbou and Cinzana are strongly overestimated. The simulated monthly AODs are significantly correlated with the measured ones ( $R = 0.57$  with  $n = 36$ ). The correlation coefficient increases up to 0.68 ( $n = 32$ ) and the slope of the linear regression is 0.99 when excluding from the comparison the November and December monthly data from Banizoumbou and Cinzana. The normalized mean error ( $NME = 100 * \frac{\sum_n |\text{Mod} - \text{Meas}|}{\sum_n \text{Meas}}$ ) is 51% for the 36 monthly data but it decreases to 32% when excluding the November and December monthly means from Banizoumbou and Cinzana.

The level of agreement between the simulated and measured surface concentration is not expected to be as high as for AODs. Indeed, the simulated “surface” concentration is an average concentration in a well-mixed layer of 54 m height while surface  $PM_{10}$  measurements are concentrations measured close to the surface ( $\sim 6$  m). Marticorena et al. (2010) show that surface concentrations measured along the SDT are

## Simulation of the mineral dust content over Western Africa

C. Schmechtig et al.

Title Page

Abstract

Introduction

Conclusions

References

Tables

Figures

◀

▶

◀

▶

Back

Close

Full Screen / Esc

Printer-friendly Version

Interactive Discussion



## Simulation of the mineral dust content over Western Africa

C. Schmechtig et al.

Title Page

Abstract

Introduction

Conclusions

References

Tables

Figures

◀

▶

◀

▶

Back

Close

Full Screen / Esc

Printer-friendly Version

Interactive Discussion



strongly impacted by local convective events at the beginning of the wet season, while median concentration are almost insensitive to the influence of these short duration events. To minimize the influence of the extreme local events, the median simulated concentrations have been compared to measurements (Fig. 10). As expected, the simulated monthly surface concentrations are much lower than the measured ones in Banizoumbou and Cinzana. Surprisingly, they are higher than the measured concentrations in M'Bour. In addition, the two monthly maximum appears as slightly shifted ( $\sim$  one month) compared to the observations. Since the simulated AODs fit well the measured AOD, this suggests a bias in the vertical distribution of the transported dust. The strong overestimation of the AODs in November and December is associated with strongly overestimated surface concentrations only at the station of Banizoumbou, while in Cinzana the simulated concentration are in the same order of magnitude than the measured ones. At the three stations, the temporal pattern and the timing of the monthly maximum of surface concentrations are in good agreement with the measurements. The simulated monthly median concentrations are significantly correlated to the measured ones ( $R = 0.50$  with  $n = 36$ ), with a normalized mean error of 82%.

These comparisons show that the model correctly captures the seasonality of the atmospheric dust load at the regional scale and the range of measured AOD and surface concentrations. The AOD are quantitatively better retrieved, since the simulated and modelled AOD are strictly comparable. The level of agreement is lower for the surface concentrations, since the measured surface concentrations are compared with the concentrations simulated in the first layer of the model (54 m), while the assumption of a well-mixed layer may not always be valid.

### 3.2.2 Daily scale

Comparisons between simulations and observations at a daily scale allow to evaluate the capability of the model to reproduce the intensity and the frequency of the single dust events contributing to the monthly mean atmospheric dust load.

The AOD simulated with CHIMERE-DUST with a one hour time step have been compared the hourly measured AOD at the three stations of the SDT (Fig. 11).

Consistently with the seasonal cycle of the monthly mean AOD, most of the peaks in AOD are observed in winter and spring in Banizoumbou and Cinzana, but later in the summer in M'Bour. These intense dust events leads to AOD generally higher than 0.5 and can reach AOD up higher than 3 at their maximum. The measured AOD tends to be higher in Banizoumbou than in Cinzana and higher in Cinzana than in M'Bour. At the three stations, most of the observed peaks in AOD are well reproduced by the model in terms of timing and intensity. The only exception is the month of November and December where moderated dust events recorded in Banizoumbou and Cinzana are strongly overestimated by the model. The major simulated dust source at this season is the region of the Bodélé Depression. The overestimation of the AODs in November and December suggest that the correction of the surface wind in this region is too strong at this period. In Banizoumbou and Cinzana, the maximum monthly mean at the end of winter is explained by a very large peak corresponding to the March 2006 dust storm (~Julian day 60). During this dust event, the simulated AOD reaches a maximum of 4 in Banizoumbou in agreement with observations. In Cinzana the maximum AOD (~2) is slightly underestimated compared to the measurements (~3). The simulation of this specific event will be further detailed in Sect. 3.3.1. During spring, several peaks, less intense, occur and for which the AOD are well captured by the model in Banizoumbou (between 1 and 2) and in Cinzana (~1) with the correct timing, for example on 31 March and 20 April in Banizoumbou and Cinzana and on 20 May in Banizoumbou. At this season, the gradient in AOD observed from Banizoumbou to Cinzana is well reproduced by the model. The spring period ends with a relatively long dust transport event (~10 days) at the beginning of June, remarkably well reproduced by the model in the three stations in terms of magnitude and duration, as further described in Sect. 3.3.2.

In M'Bour, in the spring, the AODs tends to be overestimated by the model. The highest AOD is measured during the March dust storm. The timing of this event is well captured by the model. However, the maximum simulated AOD is 7.4, while the

## Simulation of the mineral dust content over Western Africa

C. Schmechtig et al.

Title Page

Abstract

Introduction

Conclusions

References

Tables

Figures

◀

▶

◀

▶

Back

Close

Full Screen / Esc

Printer-friendly Version

Interactive Discussion



measured AOD is  $\sim 3$ . However, it is lower than the AOD simulated by Schepanski et al. (2009) or Menut et al. (2009) for the same event. Two dust events of low intensity (AOD < 1) are also measured before and after 10 April, but the corresponding simulated AOD are overestimated by a factor 2.

5 During summer, high AODs are recorded in Banizoumbou and Cinzana but the duration of the events is shorter than during spring. Only a few of these events are recorded in M'Bour. This may correspond to local dust emissions and transport by meso-scale convective systems, as described by Marticorena et al. (2010). Such meteorological systems are not correctly simulated by global meteorological models. So the ECMWF  
10 meteorological forcing used for the simulation does not allow to reproduce the impact of these systems on the dust concentrations. Several dust events occur between June and September, when dust sources located close to the North of the Senegal, in Mauritania and in Western Sahara are activated (Fig. 8b and c). The timing of these events is well reproduced or only slightly in advance compared to measurements. For these  
15 events, the simulated AOD are in agreement with the measured ones. Finally, in December, the AODs associated to the dust events are not overestimated by the model in M'Bour compared to Banizoumbou and Cinzana.

The correlation between the simulated hourly AODs and the measured ones increases as a function of the distance to the main dust sources, i.e. from Banizoumbou to M'Bour. The correlation coefficient (Normalised Mean Error) increases (decreases)  
20 from Banizoumbou ( $R = 0.44$ , NME = 82%; with  $n = 1950$ ) to Cinzana ( $R = 0.49$ , NME = 61% with  $n = 1606$ ) and M'Bour ( $R = 0.64$ , NME = 57%, with  $n = 1899$ ). The slope of the linear regression is close to 1 in Banizoumbou (0.99) and M'Bour (1.07) but much lower in Cinzana (0.60).

25 The daily median concentrations in the first layer of the model are superimposed to the daily median surface concentrations measured at the three stations on Fig. 12. The simulated surface concentrations exhibit the same order of magnitude than the measured ones. In particular the maximum simulated surface concentrations are as high as the measured ones, i.e. from 1000 to 4000  $\mu\text{g m}^{-3}$  in Banizoumbou. Note that if

## Simulation of the mineral dust content over Western Africa

C. Schmechtig et al.

Title Page

Abstract

Introduction

Conclusions

References

Tables

Figures

◀

▶

◀

▶

Back

Close

Full Screen / Esc

Printer-friendly Version

Interactive Discussion



---

**Simulation of the mineral dust content over Western Africa**

---

C. Schmechtig et al.

---

[Title Page](#)[Abstract](#)[Introduction](#)[Conclusions](#)[References](#)[Tables](#)[Figures](#)[⏪](#)[⏩](#)[◀](#)[▶](#)[Back](#)[Close](#)[Full Screen / Esc](#)[Printer-friendly Version](#)[Interactive Discussion](#)

the peaks are well reproduced, background concentrations are much lower for the simulations than for the measurements. Like for the AOD, the temporal variability of the dust concentrations at the annual scale is realistically simulated at the three stations, except in January where the model simulates extremely low concentrations (lower than  $10 \mu\text{g m}^{-3}$ ). The maximum concentrations recorded during the March dust storm are reasonably well reproduced in terms of timing. From June to September, the modelled concentrations are in the same range than the measured daily median concentrations, indicating that, except for convective situations, the model correctly reproduce the observed decrease of the concentrations during the rainy season. Surprisingly, the surface concentrations in Banizoubou and Cinzana during the dust events recorded in December are in good agreement with the measurements, while the simulated AOD were clearly overestimated compared to sunphotometer measurements.

The correlation coefficients between the simulated and measured daily median concentrations are 0.54 in Banizoumbou ( $n = 333$ ), 0.57 in Cinzana ( $n = 352$ ) and 0.44 in M'Bour. The Normalized Mean Errors ranges from 75% in Cinzana to 121% in M'Bour, with an intermediate value of 95% in Banizoumbou. The simulated concentration are thus in fair agreement with the measurements and clearly unestimated. The level of agreement between the simulated and measured concentration does not exhibit the same spatial pattern than the AOD, i.e. an increase of the level of correlation with the distance from the source regions. This suggests some bias in the simulated dust vertical distribution.

### 3.3 Typical dust events

To further investigate the model performances, we then focus on two typical events observed in March and June 2006 in Banizoumbou for which quantitative information on the altitude of the dust layers is available.

### 3.3.1 A typical low layer transport case: the March 2006 dust storm

In March 2006, a continental dust storm affects the whole Sahara and West Africa. This dust storm was initiated by a cold front in the south of the Atlas that progressed southward and westward, producing dust all along its path (Slingo et al., 2006). It produces extremely intense dust concentrations observed between 8 March and 10 March in the three stations of the Sahelian dust transect (Marticorena et al., 2010).

Once again, both the AOD and surface concentrations measured along the SDT have been compared to the simulations from 1 March to the 31 March.

The AODs (Fig. 13) and the concentrations (Fig. 14) measured during this event exhibit a similar temporal pattern, suggesting that most of the dust transport occurs in a well mixed low layer. In Banizoumbou, the more severe dust conditions (concentrations higher than  $1000 \mu\text{g m}^{-3}$ ) are recorded between 7 and 10 March, with a sharp increase of the concentration and of the AOD in the morning of 7 March and two successive sharp peaks on the 8th and 9th and a larger one on the 10th. The simulated concentrations exhibit a first but moderate increase on the 8th and two major increases on the 9th and 11th march. The first increase is much lower than the observed one and it is not associated with a peak in the AOD. The simulated maximum AODs (3.8 and 3.7) are close to the maximum measured AODs (4.2) but they remains higher than 1 for a longer period than the observed AODs. On the opposite, the maximum simulated surface concentrations ( $1386$  and  $1500 \mu\text{g m}^{-3}$ ) are lower than the measured maximum (from  $2747$  up to  $4800 \mu\text{g m}^{-3}$ ). After 11 March, the simulated AODs are overestimated compared to the observed one, while the surface concentrations are of the same order of magnitude than the measured ones. Compared to the observations, the simulated dust event is delayed of about 20 h. Despite this shift, the temporal variations of the surface concentrations are remarkably well reproduced by the model, not only for this event but for the whole month. This delay in the maximum of AOD and concentration and their underestimations suggest that the dust mobilization occurs too late in the simulations and may not be sufficiently intense. A comparable delay was obtained by

## Simulation of the mineral dust content over Western Africa

C. Schmechtig et al.

Title Page

Abstract

Introduction

Conclusions

References

Tables

Figures

⏪

⏩

◀

▶

Back

Close

Full Screen / Esc

Printer-friendly Version

Interactive Discussion



Stanelle et al. (2010) who simulated the same dust event with the COSMO-ART model forced by the analyses of the Integrated Forecast Systems from ECMWF; i.e. similar meteorological fields than the one used in this work.

One day later than in Banizoumbou, the dust event reaches the station of Cinzana, producing maximum AODs of 3 and 3.4 and surface concentrations as high as 3250 and 2900  $\mu\text{g m}^{-3}$  (Figs. 13b and 14b). Both the simulated maximum AODs and concentration are slightly lower than the observations (2.2 and 1.9 for the AOD and 1400 and 690  $\mu\text{g m}^{-3}$  for the surface concentrations). In this case, the first simulated peak is delayed of 4 h only and the duration of the events is similar to the observed one. In M'Bour, the timing and duration of the dust events is well reproduced. The simulated AOD reaches a maximum of 7.4 (Fig. 13c), while the available measurements do not exceed 2.6. But the simulated AODs coinciding with available measurements are in reasonable agreement with the observations. M'Bour is the only station where the simulated concentrations are higher than the observations (Fig. 14c).

During this event, several dust clouds are successively activated and spread over the Sahara, progressing southward, to finally produce a huge continental dust cloud. The examination of SEVIRI (Spinning Enhanced Visible and Infrared Imager) special dust products from EUMETSAT (European Organisation for the Exploitation of Meteorological Satellites) shows the activation of different dust sources affecting the different stations (Marticorena et al., 2010). On 7 March 2006, the station of Banizoumbou is overpassed by a North-eastern dust plume, while another dust plume is located North-West of the station of Cinzana. A dust cloud is also visible North-East of M'Bour that progressively moved south-westward. These differences in the source locations and emission timing explain the different levels of agreement between the simulations and the observations at the three stations.

This event has been simulated by several authors using mesoscale meteorological models (Tulet et al., 2008; Schepanski et al., 2009; Stanelle et al., 2010) and with the CHIMERE-DUST model in forecast mode (Menuet et al., 2009). The AOD measured in Banizoumbou is correctly reproduced with the meteorological model Meso-NH model

## Simulation of the mineral dust content over Western Africa

C. Schmechtig et al.

Title Page

Abstract

Introduction

Conclusions

References

Tables

Figures



Back

Close

Full Screen / Esc

Printer-friendly Version

Interactive Discussion



## Simulation of the mineral dust content over Western Africa

C. Schmechtig et al.

Title Page

Abstract

Introduction

Conclusions

References

Tables

Figures

◀

▶

◀

▶

Back

Close

Full Screen / Esc

Printer-friendly Version

Interactive Discussion



coupled with the DEAD dust emission and deposition model (Tulet et al., 2008). On the opposite, they are strongly overestimated ( $>10$ ) in Banizoumbou and Cinzana ( $>10$ ) using the dust transport model LM-MUSCAT (Schepanski et al., 2009). A similar over-estimation is obtained with the CHIMERE-DUST model run in forecast mode using the MM5 model forced by the NCEP global meteorological fields (Menut et al., 2009). However, the surface concentrations with the CHIMERE-DUST model in forecast mode at the three stations (Menut et al., 2009) have the same order of magnitude than in this work.

Figure 15 reports the vertical distribution of the simulated dust concentrations from 9 to 12 March 2006. The first peak in AOD and surface concentrations is simulated on the 9 March. The vertical profile on 9 March at 12:00 clearly shows the development of a heavily loaded dust layer between 0 and 2000 m, with a maximum around 300 m. From 9 to 11 March, the surface concentration increases to more than  $1500 \mu\text{g m}^{-3}$  while the depth of the layer extends up to 2000 m. After 11 March the dust concentration progressively decreases, in particular close to the surface. On 12 March at 12:00, the maximum dust concentration is located around 1600 m. The dust layer depth never exceeds 2000 m during this dust event, and the simulated maximum dust concentrations are always located below 1600 m.

The analysis of the vertical profile of temperature and humidity derived from radio sounding for this event revealed a well-mixed layer extending from the surface up to 860 hPa ( $\sim 1500$  m in standard atmosphere (Slingo et al., 2008)). The vertical profiles of the backscatter coefficient, measured by the lidar of the US Atmospheric Radiation Measurement (ARM) Mobile facility located in Niamey (Niger) in 2006, indicates an intense backscatter in this layer due to the presence of mineral dust (Slingo et al., 2008). These observations show that this dust event is a low layer transport whose altitude is correctly simulated by the model.

### 3.3.2 A high altitude transport layer case: 10–14 June 2006 Saharan dust transport

During the period from 10 to 20 June 2006, AODs up to 2.5 are recorded over Bani-zoumbou (Fig. 16). This increase in the AOD corresponds to the arrival of a dust event  
5 originating from the Northern Sudan and Chad (Flamant et al., 2007). From satellite observations (OMI aerosol index; MODIS Deep Blue AOD), the largest aerosol loads are observed east of Niger on June 9 but the dust plume is progressively advected westward between 9 to 14 June (Flamant et al., 2007).

On 9 June, very low surface concentrations are recorded due to precipitations following the passage of a convective system (Fig. 17). Surface concentrations remain extremely low until the arrival of the Saharan dust event as indicated by the rapid increase of the AOD on 10 June. The  $PM_{10}$  surface concentrations progressively increase from about  $20 \mu\text{g m}^{-3}$  to reach  $500 \mu\text{g m}^{-3}$  on 13 and 14 June. The measurements reported on Figs. 16 and 17, clearly show a decoupling in the temporal of the AODs and of the  
15  $PM_{10}$  surface concentration, suggesting a high altitude transport.

During this event, the comparison between the simulated and measured AOD (Fi. 15) are in good agreement. From 8 to 10 June, the measured AOD raises from 0.3 to 2.8 in agreement with the simulated AOD (0.3 to 2.1). The simulated AOD are as high as 4 11 on June but no AOD measurements are available for this day. From 12 to 16 June, the measured AOD range from 1.2 to 2.7 while the simulated AOD are between 2 and 3,  
20 i.e. slightly higher than the measured ones. However during the whole dust event, the temporal pattern of the simulated AOD are in the same range than the sunphotometer measurements. It can be noted that the maximum AODs are simulated during the night, when the sunphotometer cannot provide AOD measurements.

The measured  $PM_{10}$  surface concentrations during this period are also well simulated in terms of concentration range and in term of temporal variations (Fig. 17). The simulated dust concentrations reproduced the increase in concentration observed between 10 and 14 June with a correct magnitude and timing of the maximum concentration.  
25

## Simulation of the mineral dust content over Western Africa

C. Schmechtig et al.

Title Page

Abstract

Introduction

Conclusions

References

Tables

Figures

◀

▶

◀

▶

Back

Close

Full Screen / Esc

Printer-friendly Version

Interactive Discussion



## Simulation of the mineral dust content over Western Africa

C. Schmechtig et al.

Title Page

Abstract

Introduction

Conclusions

References

Tables

Figures

⏪

⏩

◀

▶

Back

Close

Full Screen / Esc

Printer-friendly Version

Interactive Discussion



The evolution of the altitude of dust transport simulated in Banizoumbou from 9 to 15 June (at 12:00 TU), is illustrated in Fig. 18. A low concentration dust layer is initially simulated between 4 and 6 km height on 9 June. On 10 June, the maximum concentration is located at 5 km, and the layer tends to extend downward. This also corresponds to the maximum simulated AOD. After 10 June, the dust layer peaks between 2 and 4 km, with a maximum simulated concentration ( $1200 \mu\text{g m}^{-3}$ ) at about 3000 m on 12 June. No lidar measurements from the ARM mobile facility have been published for this period. However, 13 June is the first day of 2006 for which vertical profiles from the CALIPSO (Cloud-Aerosol Lidar and Infrared Pathfinder Satellite Observations) spaceborne lidar are available. An aerosol layer located between 2 and 5 km is clearly identified in the CALIPSO track over Africa at the latitude of Niamey (<http://www-calipso.larc.nasa.gov/>). Consistently, the monthly mean profile derived from ground-based lidar observations performed in M'Bour also shows the presence of a high altitude dust layer from 2 to 5 km (Léon et al., 2009). These consistent observations from two independent sensors suggest that the model reproduces correctly the high altitude transport of this Saharan dust event.

## 4 Conclusions

In this work, we tested the capability of the CHIMERE-DUST model to reproduce the atmospheric dust load over the Sahelian region, especially its spatial and temporal distribution from the seasonal to the daily and event time scale. Several comparisons have been conducted, mainly based on a large data set of AOD and  $\text{PM}_{10}$  surface concentrations available for the year 2006 over an east-western transect located between  $13$  and  $14^\circ$  N.

The seasonal cycle of the AODs and surface concentration are correctly simulated at the regional scale. The level of agreement between the measured and simulated daily surface concentrations and hourly AOD can be considered as satisfying. This demonstrates the capability of the model to reproduce the observed dust load over

West Africa both at the seasonal time-scale and at the scale of the individual dust events at the regional scale.

The occurrence and timing of the dust events are generally correctly reproduced, which is quite challenging since the stations are located relatively close to the Saharan dust source regions. It was also shown that the model is able to reproduce the contrasted vertical distribution observed between late winter (low layer transport) and early summer (high altitude transport). However, different levels of agreement with the measured AODs and surface concentrations at some period of the year suggest some possible bias in the representation of the dust vertical distribution that would require a systematic comparison with measured vertical dust profiles.

If the temporal pattern and spatial distribution of the Saharan dust sources are realistically simulated, the intensity of the simulated emissions remains questionable since no direct quantitative observations are available to check their quality. The simulated dust emissions are significantly higher than those previously published for the Saharan. In particular, they differ by a factor 3 with those published by Laurent et al. (2008) using the same dust emission scheme. We show that the difference on the simulated dust emissions mainly comes from the forcing surface wind fields. A specific analysis of the quality and accuracy of the surface wind fields produced by different meteorological models or model versions (i.e. analysis versus operational products) compared to observations should be performed to provide a realistic forcing by surface winds over the Sahara.

Despite this high emission rate, the order of magnitude of both the simulated surface concentrations and aerosol optical thickness are consistent with the measurements available from Niger to Senegal. This indicates that the simulated regional dust budget remains largely under-constrained. These results highlight the need for further and deeper validation on the vertical distribution, the dust size distribution and the deposition fluxes.

## Simulation of the mineral dust content over Western Africa

C. Schmechtig et al.

Title Page

Abstract

Introduction

Conclusions

References

Tables

Figures

⏪

⏩

◀

▶

Back

Close

Full Screen / Esc

Printer-friendly Version

Interactive Discussion



*Acknowledgements.* Based on a French initiative, AMMA was built by an international scientific group and is currently funded by a large number of agencies, especially from France, UK, US and Africa. It has been the beneficiary of a major financial contribution from the European Community's Sixth Framework Research Programme. The work was supported by the "Institut National des Sciences de l'Univers" (INSU/CNRS). We acknowledge the mission scientists and Principal Investigators who provided the satellite data used in this research effort. The analysis and visualizations of these data (Figs. 6, 7, 8) were produced with the Giovanni online data system, developed and maintained by the NASA GES DISC (Acker and Leptoukh, 2007) (<http://disc.sci.gsfc.nasa.gov/giovanni/>).



The publication of this article is financed by CNRS-INSU.

## References

- Alfaro, S. C. and Gomes, L.: Modeling mineral aerosol production by wind erosion: Emission intensities and aerosol distributions in source areas, *J. Geophys. Res.*, 106, 18075–18084, 2001.
- Alfaro, S. C., Rajot, J. L., and Nickling, W.: Estimation of PM<sub>20</sub> emissions by wind erosion: Main sources of uncertainties, *Geomorphology*, 59, 63–74, 2004.
- Acker, J. G. and Leptoukh, G.: Online Analysis Enhances Use of NASA Earth Science Data, *Eos, Trans. AGU*, 88(2), 14–17, 2007.
- Bessagnet, B., Hodzic, A., Vautard, R., Beekmann, M., Cheinet, S., Honoré, C., Liousse, C., and Rouil, L.: Aerosol modeling with CHIMERE - preliminary evaluation at the continental scale, *Atmos. Environ.*, 38, 2803–2817, 2004.
- Bou Karam, D., Flamant, C., Tulet, P., Todd, M. C., Pelon, J., and Williams, E.: Dry cyclogenesis

ACPD

11, 8027–8079, 2011

## Simulation of the mineral dust content over Western Africa

C. Schmechtig et al.

Title Page

Abstract

Introduction

Conclusions

References

Tables

Figures

◀

▶

◀

▶

Back

Close

Full Screen / Esc

Printer-friendly Version

Interactive Discussion



## Simulation of the mineral dust content over Western Africa

C. Schmechtig et al.

Title Page

Abstract

Introduction

Conclusions

References

Tables

Figures

◀

▶

◀

▶

Back

Close

Full Screen / Esc

Printer-friendly Version

Interactive Discussion



and dust mobilization in the intertropical discontinuity of the West African Monsoon: A case study, *J. Geophys. Res.*, 114, D05115, doi:10.1029/2008JD010952, 2009.

Bouet, C., Cautenet, G., Washington, R., Todd, M. C., Laurent, B., Marticorena, B., and Bergametti, G.: Mesoscale modeling of aeolian dust emission during the BoDEX 2005 experiment, *Geophys. Res. Lett.*, 34, L07812, doi:10.1029/2006GL029184, 2007.

Cakmur, R. V., Miller, R. L., Perlwitz, J., Geogdzhayev, I. V., Ginoux, P., Koch, D., Kohfeld, K. E., Tegen, I., and Zender, C. S.: Constraining the magnitude of the global dust cycle by minimizing the difference between a model and observations, *J. Geophys. Res.*, 111, D06207, doi:10.1029/2005JD005791, 2006.

Callot, Y., Marticorena, B., and Bergametti, G.: Geomorphologic approach for modelling the surface features of arid environments in a model of dust emissions: application to the Sahara desert, *Geodin. Acta*, 13, 245–270, 2000.

Cavaliere O., Di Donfrancesco, G., Cairo, F., Fierli, F., Snels, M., Viterbini, M., Cardillo, F., Chatenet, B., Formenti, P., Marticorena, B. and Rajot, J. L.: The AMMA mulid network for aerosol characterization in West Africa, *Int. J. Remote Sens.*, doi:10.1080/01431161.2010.502156, in press, 2011.

d'Almeida, G. A.: A model for Saharan dust transport, *J. Clim. Appl. Meteorol.*, 25, 903–916, 1986.

d'Almeida, G. A. and Schütz, L.: Number, mass and volume distributions, of mineral aerosols and soils of Sahara, *J. Clim. Appl. Meteorol.*, 22, 233–243, 1983.

Dentener F. J., Carmichael, G. R., Zhang, Y., Lelieveld, J., and Crutzen, P.: The role of mineral aerosol as a reactive surface in the global troposphere, *J. Geophys. Res.*, 101, 22869–22889, 1996.

Duce, R. A.: Sources, distributions, and fluxes of mineral aerosols and their relationship to climate, in: *Aerosol Forcing of Climate*, edited by: Charlson, R. J. and Heintzenberg, J., Wiley, New-York, 43–72, 1995.

Flamant, C., Chaboureaud, J.-P., Parker, D. J., Taylor, C., Cammas, J.-P., Bock, O., Timouk, F., and Pelon, J.: Airborne observations of the impact of a convective system on the planetary boundary layer thermodynamics and aerosol distribution in the inter-tropical discontinuity region of the West African Monsoon, *Q. J. Roy. Meteorol. Soc.*, 133, 1175–1189, 2007.

Forêt, G., Bergametti, G., Dulac, F., and Menut, L.: An optimized particle size bin scheme for modelling mineral dust aerosols, *J. Geophys. Res.*, 111, D17310, doi:10.1029/2005JD006797, 2006.

Ginoux, P., Chin, M., Tegen, I., Prospero, J., Holben, B., Dubovik, O., and Lin, S. J.: Sources and distributions of dust aerosols simulated with the GOCART model, *J. Geophys. Res.*, 106, 20255–20273, doi:10.1029/2000JD000053, 2001.

Goudie, A. S. and Middleton, N. J.: Saharan dust storms: Nature and consequences, *Earth Sci. Rev.*, 56, 179–204, 2001.

Guelle, W., Balkanski, Y., Schulz, M., Marticorena, B., Bergametti, G., Moulin, C., Arimoto, R., and Perry, K. D.: Modeling the atmospheric distribution of mineral aerosol: comparison with ground measurements and satellite observations for yearly and synoptic time scales over the North Atlantic., *J. Geophys. Res.*, 105, 1997–2001, 2000.

Haywood, J. M., Pelon, J., Formenti, P., Bharmal, N., Brooks, M., Capes, G., Chazette, P., Chou, C., Christopher, S., Coe, H., Cuesta, J., Derimian, Y., Desboeufs, K., Greed, G., Harrison, M., Heese, B., Highwood, E. J., Johnson, B., Mallet, M., Marticorena, B., Marsham, J., Milton, S., Myhre, G., Osborne, S., Parker, D. J., Rajot, J.-L., Schulz, M., Slingo, A., Tanré, D., and Tulet, P.: Overview of the Dust and Biomass burning Experiment and African Monsoon Multidisciplinary Analysis Special Observing Period-0, *J. Geophys. Res.*, 113, D00C17, doi:10.1029/2008JD010077, 2008.

Heinold, B., Helmert, J., Hellmuth, O., Wolke, R., Ansmann, A., Marticorena, B., Laurent, B., and Tegen, I.: Regional modeling of Saharan dust events using LM-MUSCAT: Model description and case studies, *J. Geophys. Res.*, 112, D11204, doi:10.1029/2006JD007443, 2007.

Herman, J. R., Bhartia, P. K., Torres, O., Hsu, C., Sefstor, C., and Celarier, E.: Global distribution of UV-absorbing aerosols from Nimbus 7/TOMS data, *J. Geophys. Res.*, 102, 16911–16922, 1997.

Holben, B. N., Tanre, D., Smirnov, A., Eck, T. F., Slutsker, I., Abuhassan, N., Newcomb, W. W., Schafer, J., Chatenet, B., Lavenu, F., Kaufman, Y., Van de Castle, J., Setzer, A., Markham, B., Clark, D., Frouin, R., Halthore, R., Karnieli, A., O'Neill, N. T., Pietras, C., Pinker, R. T., Voss, K., and Zibordi, G.: An emerging ground-based aerosol climatology: Aerosol Optical Depth from AERONET, *J. Geophys. Res.*, 106, 12067–12098, 2001.

Hsu, N. C., Tsay, S.-C., King, M. D., and Herman, J. R.: Aerosol properties over bright-reflecting source regions, *IEEE T. Geosci. Remote*, 42(3), 557–569, 2004.

Hsu, N. C., Tsay, S.-C., King, M. D., and Herman, J. R.: Deep blue retrievals of Asian aerosol properties during ACE-Asia, *IEEE T. Geosci. Remote*, 44(11), 3180–3195, 2006.

Jaenicke, R. and Schütz, L.: Comprehensive study of physical and chemical properties of the

## Simulation of the mineral dust content over Western Africa

C. Schmechtig et al.

Title Page

Abstract

Introduction

Conclusions

References

Tables

Figures

◀

▶

◀

▶

Back

Close

Full Screen / Esc

Printer-friendly Version

Interactive Discussion



## Simulation of the mineral dust content over Western Africa

C. Schmechtig et al.

Title Page

Abstract

Introduction

Conclusions

References

Tables

Figures

◀

▶

◀

▶

Back

Close

Full Screen / Esc

Printer-friendly Version

Interactive Discussion



surface aerosols in Cape Verde Islands region, *J. Geophys. Res.*, 83, 3585–3599, 1978.

Jickells, T. D., An, Z. S., Andersen, K. K., Baker, A. R., Bergametti, G., Brooks, N., Cao, J. J., Boyd, P. W., Duce, R. A., Hunter, K. A., Kawahata, H., Kubilay, N., La Roche, J., Liss, P. S., Mahowald, N., Prospero, J. M., Ridgwell, A. J., Tegen, I., and Torres, R.: Global iron connections: Between desert dust, ocean biogeochemistry and climate, *Science*, 308, 67–71, 2005.

Koren, I. and Kaufman, Y. J.: Direct wind measurements of Saharan dust events from Terra and Aqua satellites, *Geophys. Res. Lett.*, 31, L06122, doi:10.1029/2003GL019338, 2004.

Koren, I., Kaufman, Y. J., Washington, R., Todd, M. C., Rudich, Y., Martins, J. V., and Rosenfeld, D.: The Bodélé depression: A single spot in the Sahara that provides most of the mineral dust to the Amazon forest, *Environ. Res. Lett.*, 1, 014005, doi:10.1088/1748-9326/1/1/014005, 2006.

Laurent, B., Marticorena, B., Bergametti, G., Léon, J. F., and Mahowald, N. M.: Modeling mineral dust emissions from the Sahara desert using new surface properties and soil database, *J. Geophys. Res.*, 113, D14218, doi:10.1029/2007JD009484, 2008.

Loosmore, G. and Cederwall, R.: Precipitation scavenging of atmospheric aerosols for emergency response applications: Testing an updated model with new real-time data, *Atmos. Environ.*, 38, 993–1003, 2004.

Luo, C., Mahowald, N. M., and del Corral, J.: Sensitivity study of meteorological parameters on mineral aerosol mobilization, transport, and distribution, *J. Geophys. Res.*, 108(D15), 4447, doi:10.1029/2003JD003483, 2003.

Mahowald, N. M., Jickells, T. D., Baker, A. R., Artaxo, P., Benitez-Nelson, C., Bergametti, G., Bond, T. C., Chen, Y., Cohen, D. D., Heruk, B., Kubilay, N., Losno, C. Luo, W. Maenhaut, K. A. Mc Gee, G. Okin, R. L. Seifert and S. and Tsukuda, R.: The global distribution of atmospheric phosphorus deposition and anthropogenic impacts, *Global Biogeochem. Cy.*, 22, GB4026, doi:10.1029/2008GB003240, 2008.

Manabe, Y. and Godlieb, J.: Nitrate formation on sea-salt and mineral particles – a single particle approach, *Atmos. Environ.*, 26A, 1763–1769, 1992.

Marticorena, B. and Bergametti, G.: Modelling the atmospheric dust cycle: 1. Design of a soil derived dust production scheme, *J. Geophys. Res.*, 100, 16415–16430, 1995.

Marticorena, B. and Bergametti, G.: Two-year simulations of seasonal and interannual changes of the Saharan dust emissions, *Geophys. Res. Lett.*, 23, 1921–1924, 1996.

Marticorena, B., Bergametti, G., Aumont, B., Callot, Y., N'Doumé, C., and Legrand, M.: Mod-

## Simulation of the mineral dust content over Western Africa

C. Schmechtig et al.

Title Page

Abstract

Introduction

Conclusions

References

Tables

Figures

◀

▶

◀

▶

Back

Close

Full Screen / Esc

Printer-friendly Version

Interactive Discussion



eling the atmospheric dust cycle: 2-Simulations of Saharan dust sources, *J. Geophys. Res.*, 102, 4387–4404, 1997.

Marticorena, B., Chatenet, B., Rajot, J. L., Traoré, S., Coulibaly, M., Diallo, A., Koné, I., Maman, A., NDiaye, T., and Zakou, A.: Temporal variability of mineral dust concentrations over West Africa: analyses of a pluriannual monitoring from the AMMA Sahelian Dust Transect, *Atmos. Chem. Phys.*, 10, 8899–8915, doi:10.5194/acp-10-8899-2010, 2010.

Menut, L.: Adjoint modelling for atmospheric pollution processes sensitivity at regional scale during the ESQUIF IOP2, *J. Geophys. Res.*, 108, 8562, doi:10.1029/2002JD002549, 2003.

Menut, L., Forêt, G., and Bergametti, G.: Sensitivity of mineral dust concentrations to the model size distribution accuracy, *J. Geophys. Res.*, 112, D10210, doi:10.1029/2006JD007766, 2007.

Menut, L., Chiapello, I., and Moulin, C.: Predictability of mineral dust concentrations: The African Monsoon Multidisciplinary Analysis first short observation period forecasted with CHIMERE-DUST, *J. Geophys. Res.*, 114, D07202, doi:10.1029/2008JD010523, 2009.

Moulin, C., Gordon, H. R., Banzon, V. F., and Evans, R. H.: Assessment of Saharan dust absorption in the visible from SeaWiFS imagery, *J. Geophys. Res.*, 106(D16), 18239–18249, doi:10.1029/2000JD900812, 2001.

N'Tchayi, G. M., Bertrand, J., Legrand, M., and Baudet, J.: Temporal and spatial variations of the atmospheric dust loading throughout West Africa over the last thirty years, *Ann. Geophys.*, 12, 265–273, doi:10.1007/s00585-994-0265-3, 1994.

Ogunjobi, K. O., He, Z., and Simmer, C.: Spectral aerosol optical properties from AERONET Sun-photometric measurements over West Africa, *Atmos. Res.*, 88, 89–107, 2008.

Prospero, J. M. and Nees, R. T.: Dust concentration in the atmosphere of the Equatorial North Atlantic: possible relationship to the Sahelian drought, *Science*, 196, 1196–1198, 1977.

Prospero, J. M. and Nees, R. T.: Impact of the north African drought and El Nino on mineral dust in the Barbados trade winds, *Nature*, 320, 735–738, 1986.

Prospero, J. M., Ginoux, P., Torres, O., Nicholson, S. E., and Gill, T. E.: Environmental characterization of global sources of atmospheric soil dust identified with the Nimbus 7 Total Ozone Mapping Spectrometer (TOMS) absorbing aerosol product, *Rev. Geophys.*, 40(1), 1–31, 2002.

Redelsperger, J. L., Thorncroft, C. D., Diedhiou, A., Lebel, T., Parker, D. J., and Polcher, J.: African Monsoon Multidisciplinary Analysis An International Research Project and Field Campaign, *B. Am. Meteorol. Soc.*, 87(12), 1739, doi:10.1175/BAMS-87-12-1739, 2006.

## Simulation of the mineral dust content over Western Africa

C. Schmechtig et al.

Title Page

Abstract

Introduction

Conclusions

References

Tables

Figures

◀

▶

◀

▶

Back

Close

Full Screen / Esc

Printer-friendly Version

Interactive Discussion



Schepanski, K., Tegen, I., Todd, M. C., Heinold, B., Bönisch, G., Laurent, B., and Macke, A.: Meteorological processes forcing Saharan dust emission inferred from MSG]SEVIRI observations of subdaily dust source activation and numerical models, *J. Geophys. Res.*, 114, D10201, doi:10.1029/2008JD010325, 2009.

5 Slingo, A., Ackerman, T. P., Allan, R. P., Kassianov, E. I., McFarlane, S. A., Robinson, G. J., Barnard, J. C., Miller, M. A., Harries, J. E., Russell, J. E., and Dewitte, S.: Observations of the impact of a major Saharan dust storm on the atmospheric radiation balance, *Geophys. Res. Lett.*, 33, L24817, doi:10.1029/2006GL027869, 2006.

10 Slingo, A., Bharmal, N. A., Robinson, G. J., Settle, J. J., Allan, R. P., White, H. E., Lamb, P. J., Issa Lélé, M., Turner, D. D., McFarlane, S., Kassianov, E., Barnard, J., Flynn, C., and Miller, M.: Overview of observations from the RADAGAST experiment in Niamey, Niger. Part 1: Meteorology and thermodynamic variables, *J. Geophys. Res.*, 113, D00E01, doi:10.1029/2008JD009909, 2008.

15 Sokolik, I., Winker, D., Bergametti, G., Gillette, D. A., Carmichael, G., Kaufman, Y., Gomes, L., Schütz, L., and Penner, J.: Outstanding problems in quantifying the radiative impact of mineral dust, *J. Geophys. Res.*, 106, 18075–18084, 2001.

Stanelle, T., Vogel, B., Vogel, H., Bäumer, D., and Kottmeier, C.: Feedback between dust particles and atmospheric processes over West Africa during dust episodes in March 2006 and June 2007, *Atmos. Chem. Phys.*, 10, 10771–10788, doi:10.5194/acp-10-10771-2010, 2010.

20 Swap, R., Garstang, M., Greco, S., Talbot, R., and Kållberg, P.: Saharan dust in the Amazon basin, *Tellus*, 44B, 133–149, 1992.

Tegen, I. and Fung, I.: Modeling of mineral dust in the atmosphere: Sources, transport, and optical thickness, *J. Geophys. Res.*, 99, 22897–22914, 1994.

25 Tegen, I. and Lacis, A.: Modeling of particle size distribution and its influence on the radiative properties of mineral dust aerosol, *J. Geophys. Res.*, 101, 19237–19244, 1996.

Tegen, I., Harrison, S. P., Kohfeld, K., Prentice, I. C., Coe, M., and Heimann, M.: Impact of vegetation and preferential source areas on global dust aerosol: Results from a model study, *J. Geophys. Res.*, 107(D21), 4576, doi:10.1029/2001JD000963, 2002.

30 Tegen, I., Heinold, B., Todd, M., Helmert, J., Washington, R., and Dubovik, O.: Modelling soil dust aerosol in the Bodl depression during the BoDEx campaign, *Atmos. Chem. Phys.*, 6, 4345–4359, doi:10.5194/acp-6-4345-2006, 2006.

Torres, O., Bhartia, P. K., Herman, J. R., Ahmad, Z., and Gleason, J.: Derivation of aerosol

## Simulation of the mineral dust content over Western Africa

C. Schmechtig et al.

Title Page

Abstract

Introduction

Conclusions

References

Tables

Figures

◀

▶

◀

▶

Back

Close

Full Screen / Esc

Printer-friendly Version

Interactive Discussion



properties from satellite measurements of backscattered ultraviolet radiation: Theoretical basis, *J. Geophys. Res.*, 103, 17099–17110, 1998.

Tulet, P., Mallet, M., Pont, V., Pelon, J., and Boone, A.: The 7–13 March 2006 dust storm over West Africa: Generation, transport, and vertical stratification, *J. Geophys. Res.*, 113, D00C08, doi:10.1029/2008JD009871, 2008.

Van Leer, B.: Towards the ultimate conservative difference scheme.V A second order sequel to Godunov's method, *J. Comput. Phys.*, 32, 101–136, 1979.

Vautard, R., Beekmann, M., Roux, J., and Gombert, D.: Validation of a deterministic forecasting system for the ozone concentrations over the Paris area, *Atmos. Environ.*, 35 2449–2461, 2001.

Venkatram, A. and Pleim, J.: The electrical analogy does not apply to modeling dry deposition of particles, *Atmos. Environ.*, 33, 3075–3076, 1999.

Wang, M., Knobelspiesse, K. D., and Mc Clain, C. R.: Study of the Sea-Viewing Wide Field-of-View Sensor (SeaWiFS) aerosol optical property data over ocean in combination with the ocean color products, *J. Geophys. Res.*, 110, D10S06, doi:10.1029/2004JD004950, 2005.

Washington, R., Todd, M. C., Engelstaedter, S., M'Bainayel, S., and Mitchell, F.: Dust and the low-level circulation over the Bode'le' Depression, Chad: Observations from BoDEX 2005, *J. Geophys. Res.*, 111, D03201, doi:10.1029/2005JD006502, 2006.

Wesely, M. L.: Parameterizations of surface resistance to gaseous dry deposition in regional-scale numerical models, *Atmos. Environ.*, 23, 1293–1304, 1989.

Wu, P.-M. and Okada, K.: Nature of the coarse nitrate particles in the atmosphere – A single particle approach, *Atmos. Environ.*, 28, 2053–2060, 1994.

Yoshioka, M., Mahowald, N., Dufresne, J. L., and Luo, C.: Simulation of absorbing aerosol indices for African dust, *J. Geophys. Res.*, 110, D18S17, doi:10.1029/2004JD005276, 2005.

Zhao, D., Xiong, J., Xu, Y., and Chan, W. H.: Acid rain in southern China, *Atmos. Environ.*, 22, 349–358, 1988

**Simulation of the mineral dust content over Western Africa**

C. Schmechtig et al.

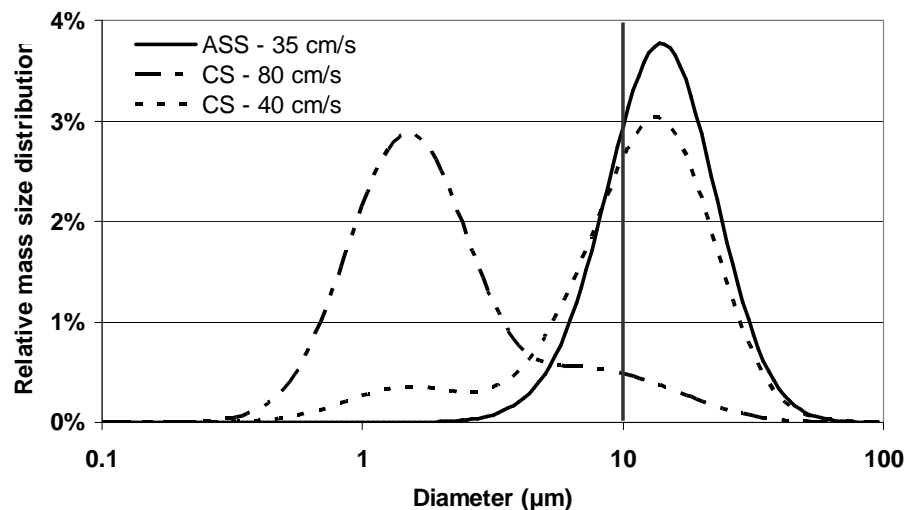


**Fig. 1.** Examples of dust mass size distributions from Alfaro and Gomes (2001) produced by two different soils (ASS: Alumino Silicated Silt; CS: Coarse Sand) at different wind friction velocity leading to different percentages (0% for ASS – 35 cm s<sup>-1</sup>; 83% for CS – 80 cm s<sup>-1</sup>; 10% for CS – 40 cm s<sup>-1</sup>) in the fine mode ( $D_{\text{med}1} = 1.5 \mu\text{m}$ ,  $\sigma_1 = 1.7$ ).

[Title Page](#)[Abstract](#)[Introduction](#)[Conclusions](#)[References](#)[Tables](#)[Figures](#)[◀](#)[▶](#)[◀](#)[▶](#)[Back](#)[Close](#)[Full Screen / Esc](#)[Printer-friendly Version](#)[Interactive Discussion](#)

**Simulation of the mineral dust content over Western Africa**

C. Schmechtig et al.

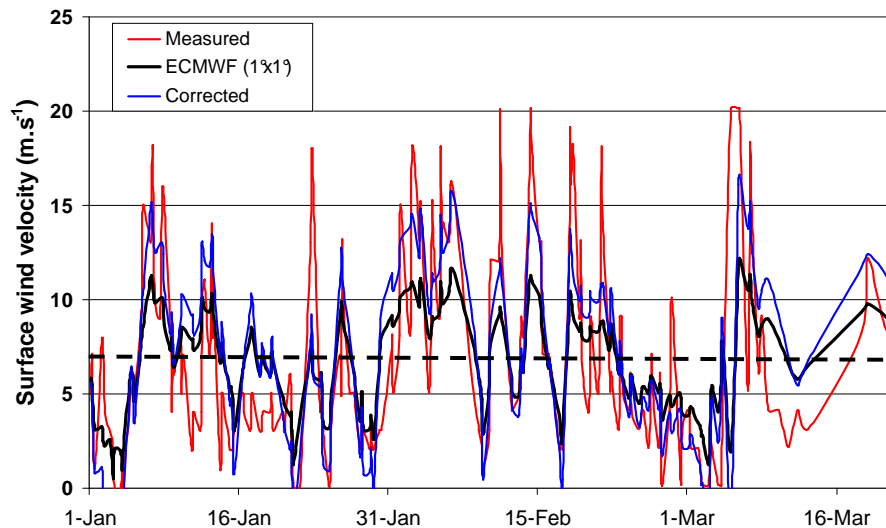


**Fig. 2.** 10 m wind velocity measured at the meteorological station of Faya-Largeau (Chad), 10 m wind velocity from the ECMWF operational products ( $1^\circ \times 1^\circ$ ) and 10 m wind velocity from ECMWF corrected using Eq. (1) in January–March 2004.

Title Page

Abstract

Introduction

Conclusions

References

Tables

Figures

◀

▶

◀

▶

Back

Close

Full Screen / Esc

Printer-friendly Version

Interactive Discussion



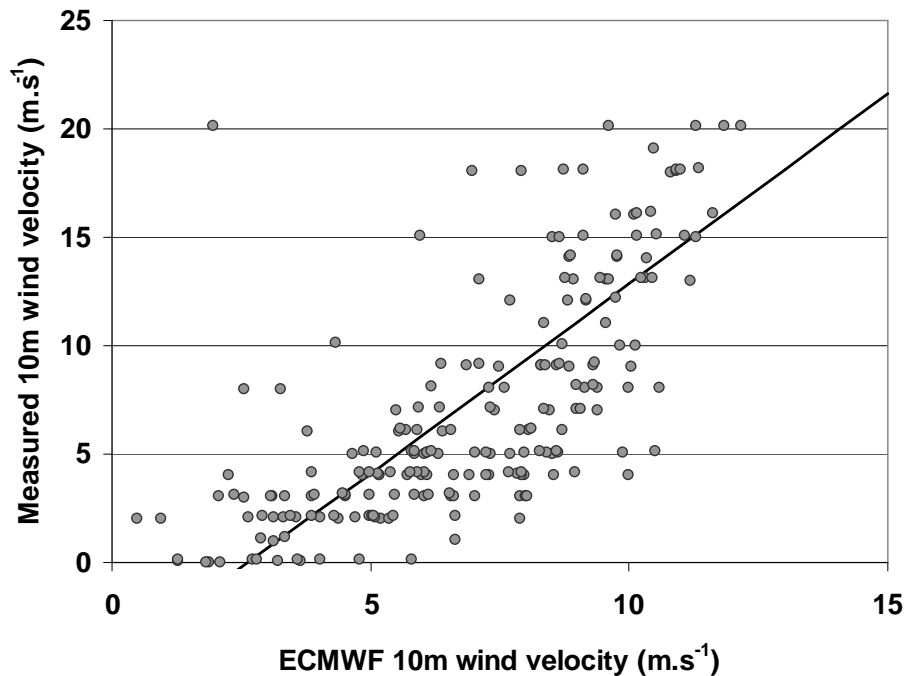


**Fig. 3.** 10 m wind velocity measured at the meteorological station of Faya-Largeau (Chad) as a function of the 10 m wind velocity from the ECMWF operational products for the square degree including the meteorological station of Faya Largeau ( $R = 0.7988$ ,  $n = 211$ ).

**Simulation of the mineral dust content over Western Africa**

C. Schmechtig et al.

Title Page	
Abstract	Introduction
Conclusions	References
Tables	Figures
◀	▶
◀	▶
Back	Close
Full Screen / Esc	
Printer-friendly Version	
Interactive Discussion	



**Simulation of the mineral dust content over Western Africa**

C. Schmechtig et al.

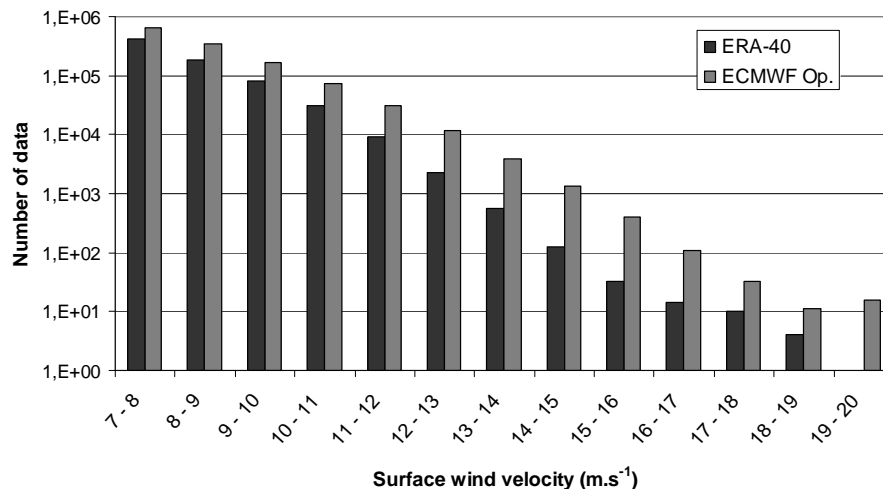


**Fig. 4.** Distribution of the surface wind velocity higher than 7 m s<sup>-1</sup> for the year 2000 for the ERA-40 data base (dark grey) and for the ECMWF operational products (light grey) over the emission domain.

Title Page

Abstract Introduction

Conclusions References

Tables Figures

◀ ▶

◀ ▶

Back Close

Full Screen / Esc

Printer-friendly Version

Interactive Discussion



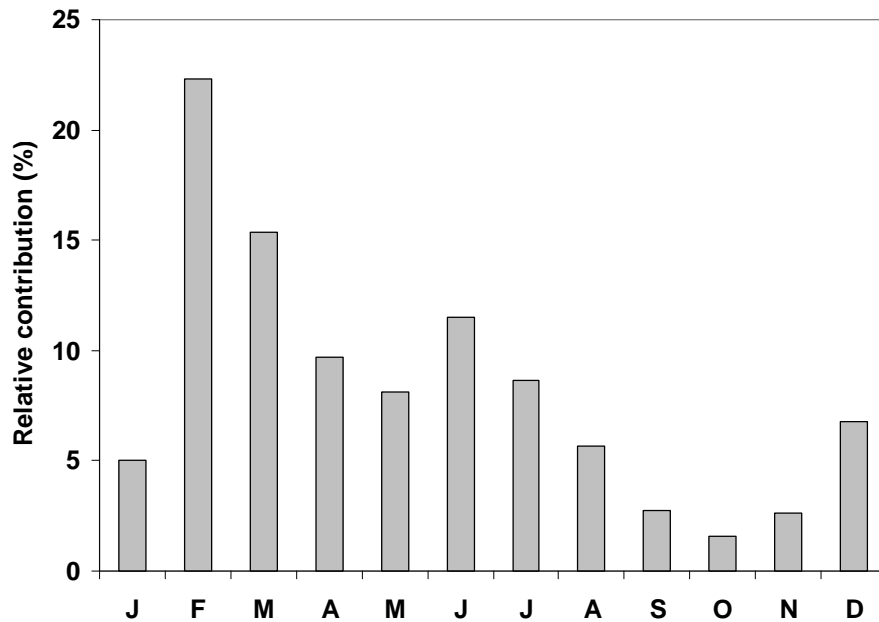


Fig. 5. Monthly relative contribution to the annual Saharan dust emissions simulated for 2006.

**Simulation of the mineral dust content over Western Africa**

C. Schmechtig et al.

Title Page

Abstract Introduction

Conclusions References

Tables Figures

◀ ▶

◀ ▶

Back Close

Full Screen / Esc

Printer-friendly Version

Interactive Discussion



## Simulation of the mineral dust content over Western Africa

C. Schmechtig et al.

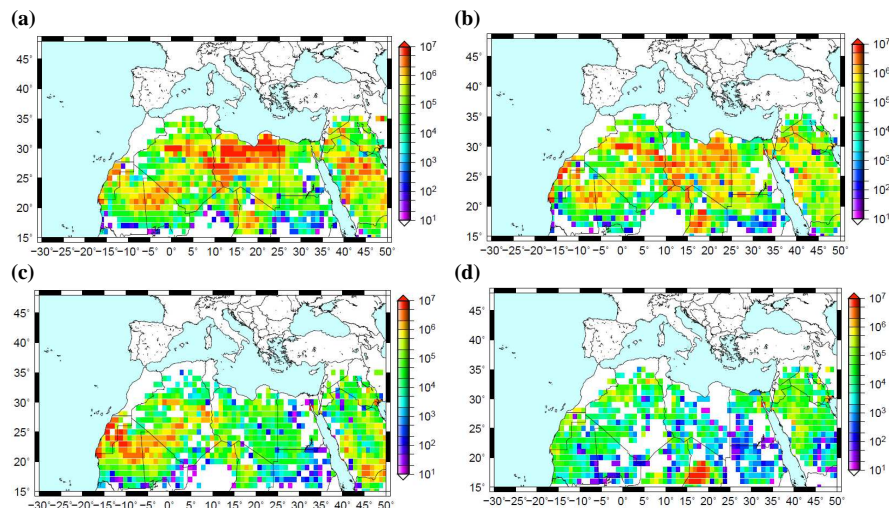


**Fig. 6.** Simulated dust emissions ( $g$ ) for **(a)** winter (January-February-March), **(b)** spring (April-May-June), **(c)** summer (July-August-September) and **(d)** autumn (October-November-December) 2006.

[Title Page](#)[Abstract](#)[Introduction](#)[Conclusions](#)[References](#)[Tables](#)[Figures](#)[◀](#)[▶](#)[◀](#)[▶](#)[Back](#)[Close](#)[Full Screen / Esc](#)[Printer-friendly Version](#)[Interactive Discussion](#)

## Simulation of the mineral dust content over Western Africa

C. Schmechtig et al.

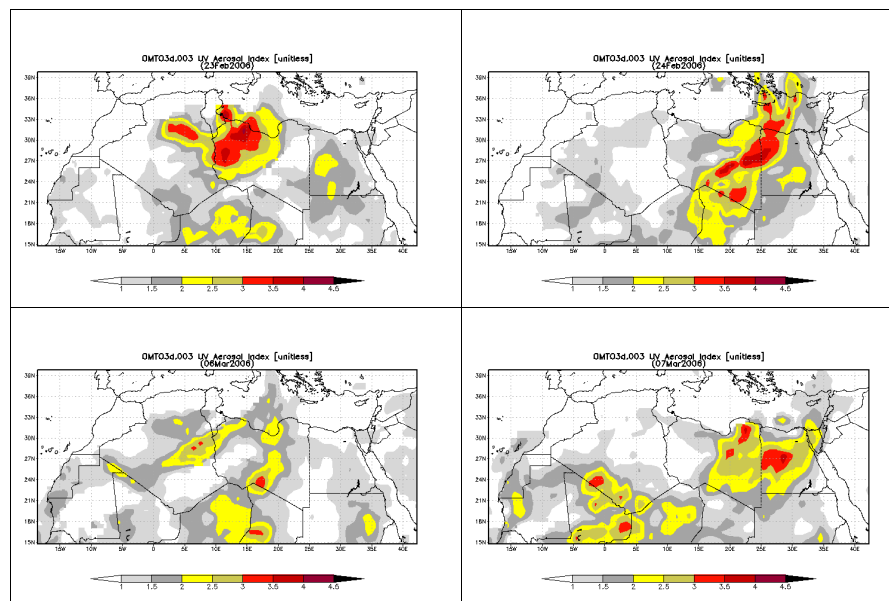


**Fig. 7.** Daily aerosol UV indexes derived from OMI satellite observations for 23 and 24 February 2006 (up) and for 6 and 7 March 2009 (down).

[Title Page](#)[Abstract](#)[Introduction](#)[Conclusions](#)[References](#)[Tables](#)[Figures](#)[◀](#)[▶](#)[◀](#)[▶](#)[Back](#)[Close](#)[Full Screen / Esc](#)[Printer-friendly Version](#)[Interactive Discussion](#)

## Simulation of the mineral dust content over Western Africa

C. Schmechtig et al.

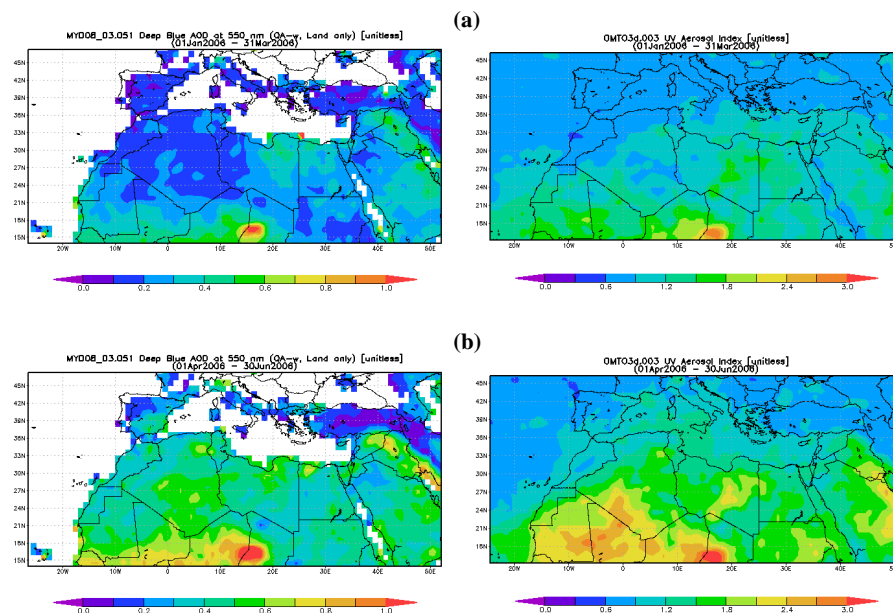


**Fig. 8.** Seasonal mean MODIS Deep Blue AOD (right) and OMI Aerosol Index (left) for **(a)** January-February-March 2006, **(b)** April-May-June 2006.

[Title Page](#)
[Abstract](#)
[Introduction](#)
[Conclusions](#)
[References](#)
[Tables](#)
[Figures](#)
[◀](#)
[▶](#)
[◀](#)
[▶](#)
[Back](#)
[Close](#)
[Full Screen / Esc](#)
[Printer-friendly Version](#)
[Interactive Discussion](#)


## Simulation of the mineral dust content over Western Africa

C. Schmechtig et al.

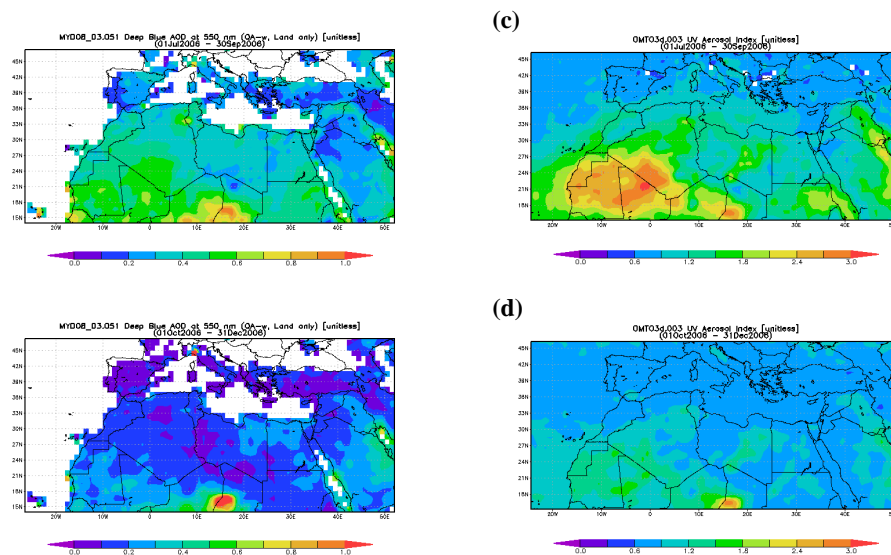


**Fig. 8.** Seasonal mean MODIS Deep Blue AOD (right) and OMI Aerosol Index (left) for **(c)** July-August-September and **(d)** October-November-December 2006.

Title Page

Abstract

Introduction

Conclusions

References

Tables

Figures

◀

▶

◀

▶

Back

Close

Full Screen / Esc

Printer-friendly Version

Interactive Discussion



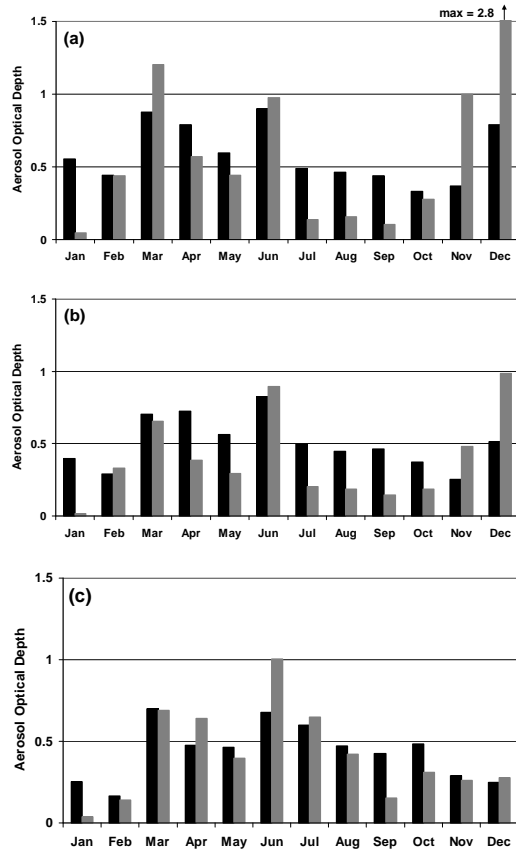


**Fig. 9.** Monthly mean aerosol optical depths measured by the AERONET sunphotometers (675 nm ; level2) for  $\alpha < 0.4$  (black) and monthly mean coinciding simulated AOD (550 nm) (grey) for **(a)** Banizoumbou (Niger), **(b)** Cinzana (Mali) and **(c)** M'Bour (Senegal) in 2006.

**Simulation of the mineral dust content over Western Africa**

C. Schmechtig et al.

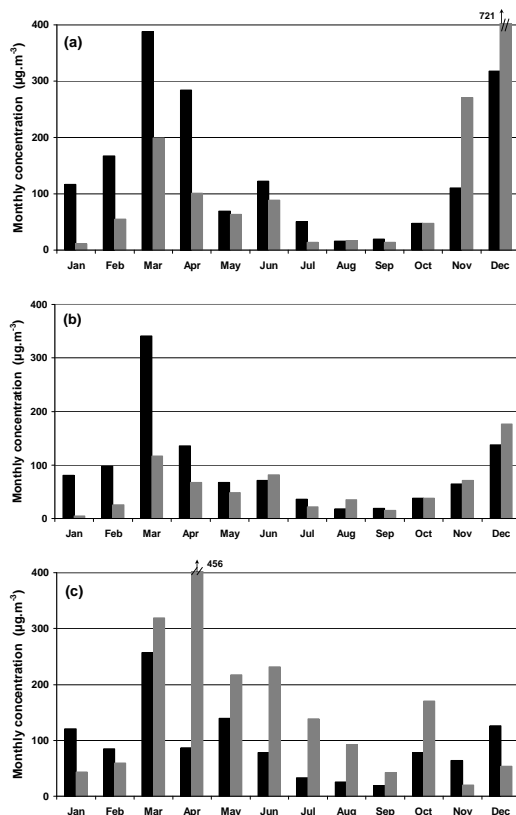


**Fig. 10.** Monthly mean of daily median measured (black) and simulated (grey) surface concentrations in **(a)** Banizoumbou (Niger), **(b)** Cinzana (Mali) and **(c)** M'Bour (Senegal).

Title Page

Abstract

Introduction

Conclusions

References

Tables

Figures

◀

▶

◀

▶

Back

Close

Full Screen / Esc

Printer-friendly Version

Interactive Discussion



## Simulation of the mineral dust content over Western Africa

C. Schmechtig et al.

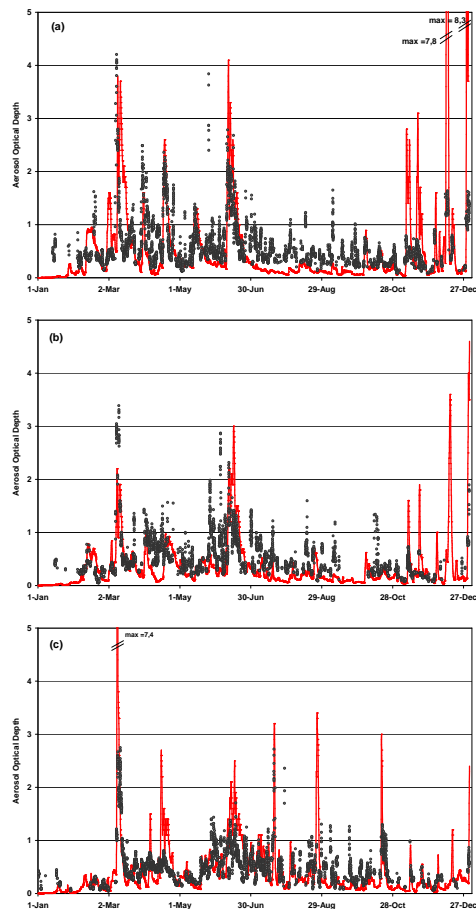


**Fig. 11.** Measured aerosol optical depth (level 2 data @675 nm at nominal time resolution) with  $\alpha < 0.4$  (grey circles) and hourly simulated aerosol optical depth (@550 nm) (red line) in **(a)** Banizoumbou (Niger), **(b)** Cinzana (Mali) and **(c)** M'Bour (Senegal) in 2006.

[Title Page](#)[Abstract](#)[Introduction](#)[Conclusions](#)[References](#)[Tables](#)[Figures](#)[◀](#)[▶](#)[◀](#)[▶](#)[Back](#)[Close](#)[Full Screen / Esc](#)[Printer-friendly Version](#)[Interactive Discussion](#)

## Simulation of the mineral dust content over Western Africa

C. Schmechtig et al.

Title Page

Abstract

Introduction

Conclusions

References

Tables

Figures

◀

▶

◀

▶

Back

Close

Full Screen / Esc

Printer-friendly Version

Interactive Discussion

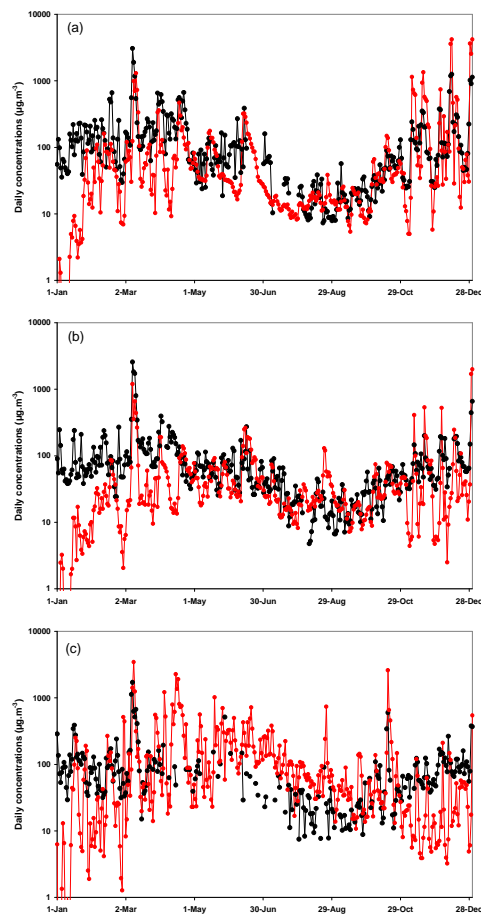


**Fig. 12.** Daily median measured (black dots) and simulated (grey dots)  $PM_{10}$  surface concentrations in **(a)** Banizoumbou (Niger), **(b)** Cinzana (Mali) and **(c)** M'Bour (Senegal) in 2006.

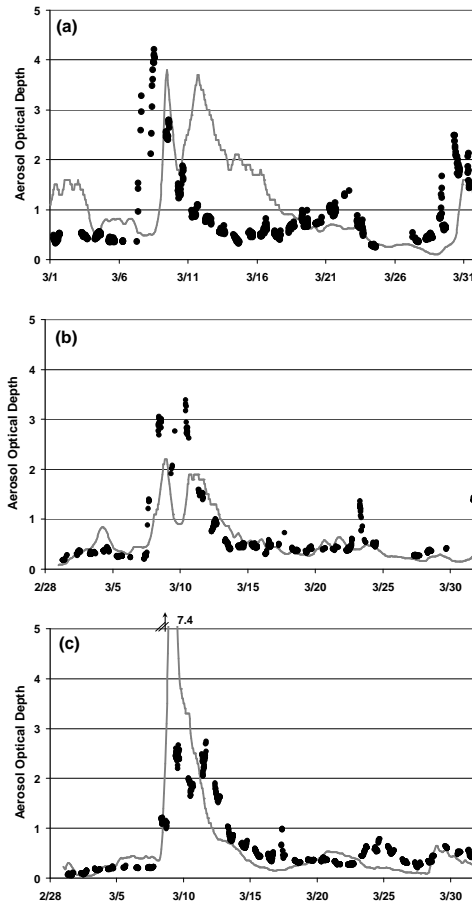


**Fig. 13.** Measured (black dots: AERONET level 2 data @675 nm) and simulated (grey line) hourly Aerosol Optical Depth (@550 nm) over **(a)** Banizoumbou (Niger), **(b)** Cinzana (Mali) and **(c)** M'Bour (Senegal) in March 2006.

**Simulation of the mineral dust content over Western Africa**

C. Schmechtig et al.

Title Page

Abstract Introduction

Conclusions References

Tables Figures

◀ ▶

◀ ▶

Back Close

Full Screen / Esc

Printer-friendly Version

Interactive Discussion



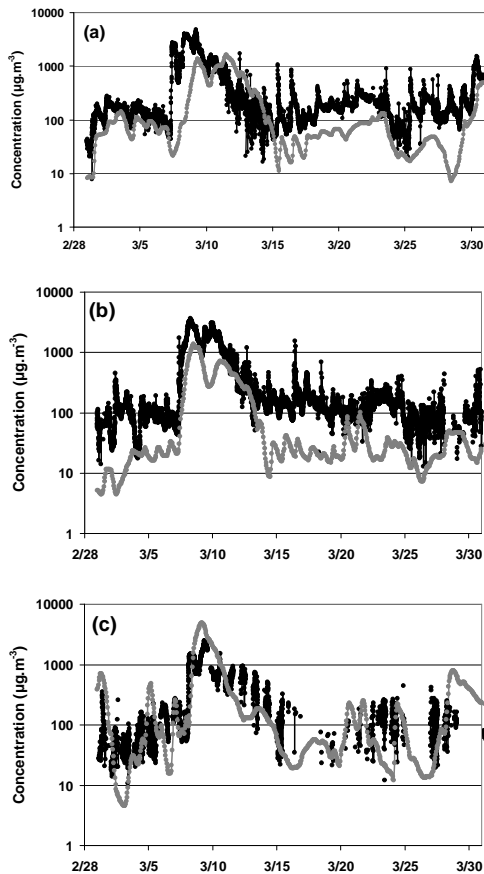


**Fig. 14.** Measured (black dots) and simulated daily  $PM_{10}$  surface concentrations in **(a)** Bani-zoumbou (Niger), **(b)** Cinzana (Mali) and **(c)** M'Bour (Senegal) in March 2006.

## Simulation of the mineral dust content over Western Africa

C. Schmechtig et al.

Title Page

Abstract

Introduction

Conclusions

References

Tables

Figures

◀

▶

◀

▶

Back

Close

Full Screen / Esc

Printer-friendly Version

Interactive Discussion





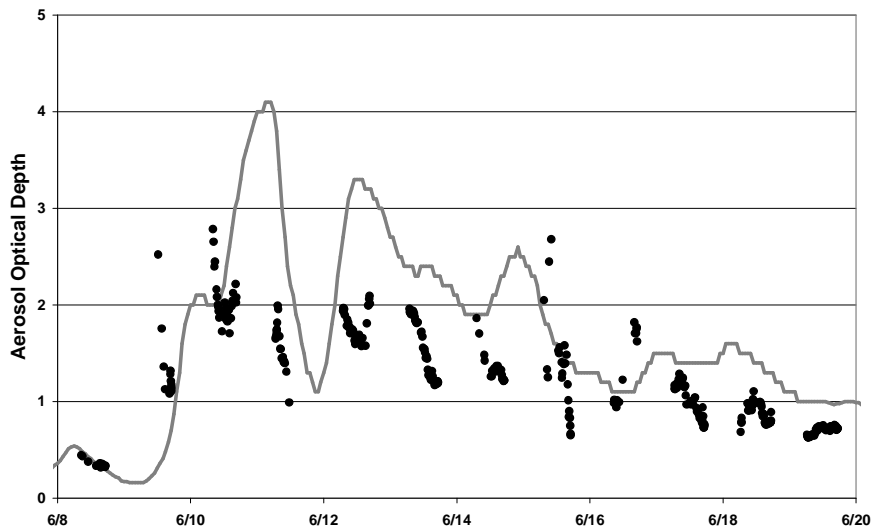


**Fig. 16.** Measured (AERONET level 2 data @675 nm) (black dots) and simulated hourly (@550 nm) (grey line) Aerosol Optical Depth over Banizoumbou (Niger) from 8 June 2006 to 20 June 2006.

**Simulation of the mineral dust content over Western Africa**

C. Schmechtig et al.

Title Page

Abstract Introduction

Conclusions References

Tables Figures

◀ ▶

◀ ▶

Back Close

Full Screen / Esc

Printer-friendly Version

Interactive Discussion



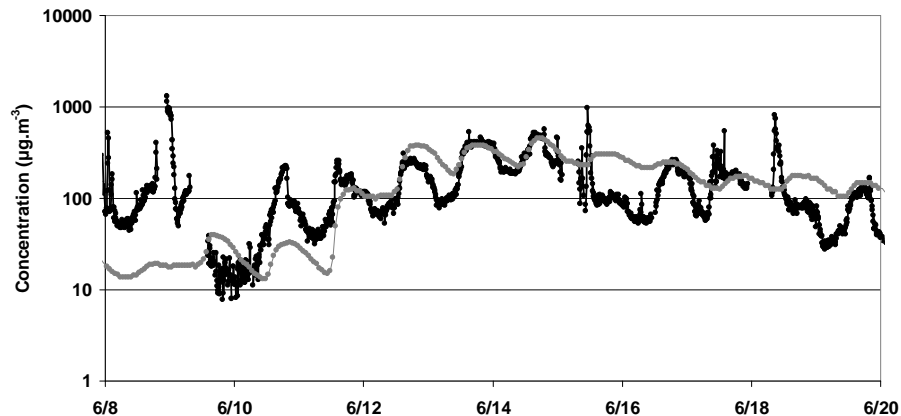


**Fig. 17.** Measured (black dots) and simulated (grey dots)  $PM_{10}$  dust surface concentrations in Banizoumbou (Niger) from 8 June 2006 to 20 June 2006.

**Simulation of the mineral dust content over Western Africa**

C. Schmechtig et al.

Title Page

Abstract Introduction

Conclusions References

Tables Figures

◀ ▶

◀ ▶

Back Close

Full Screen / Esc

Printer-friendly Version

Interactive Discussion



## Simulation of the mineral dust content over Western Africa

C. Schmechtig et al.

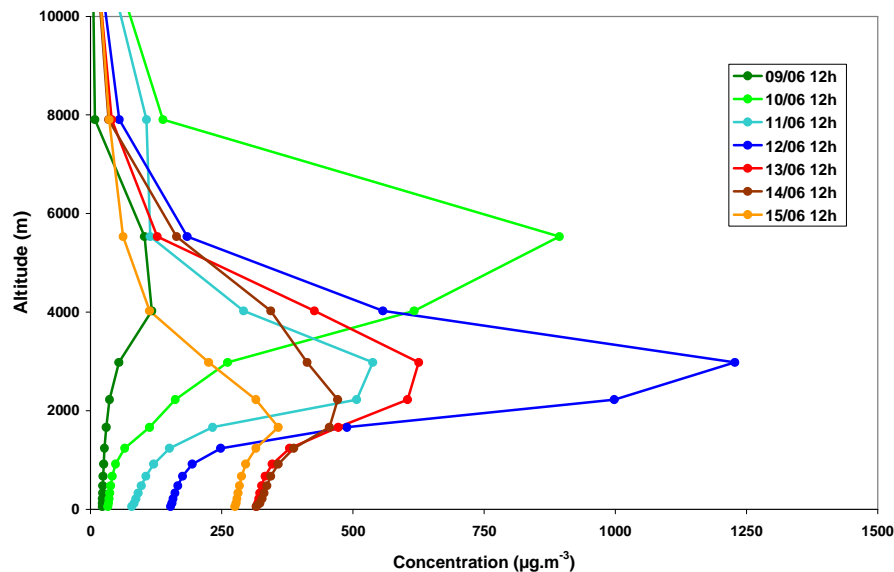


**Fig. 18.** Vertical distribution of the simulated mass concentration in Banizoumbou (Niger) in June 2006.

[Title Page](#)[Abstract](#)[Introduction](#)[Conclusions](#)[References](#)[Tables](#)[Figures](#)[◀](#)[▶](#)[◀](#)[▶](#)[Back](#)[Close](#)[Full Screen / Esc](#)[Printer-friendly Version](#)[Interactive Discussion](#)